

Novel Benzoic Acid Congeners of Bilirubin

Stefan E. Boiadjev and David A. Lightner*

Chemistry Department, University of Nevada, Reno, Nevada 89557

lightner@scs.unr.edu

Received March 13, 2003

Three regioisomeric bilirubins and biliverdins with propionic acids replaced by benzoic acids were synthesized from the corresponding xanthobilirubic acids by oxidative coupling. The rubins were found to exhibit widely varying polarity, spectroscopic properties, and stereochemistry. The isomer with *ortho* benzoic acids (**1o**) was much less polar than either the *meta* (**1m**) or *para* (**1p**) because **1o** (but not **1m** and **1p**) can adopt a folded conformation with both carboxylic acids intramolecularly hydrogen bonded to the opposing dipyrinones. The consequences of such conformational differentiation are found in the varying ¹H NMR, UV–vis, and circular dichroism spectral properties.

Introduction

Jaundice appears in humans who cannot efficiently eliminate bilirubin (Figure 1), which is a yellow tetrapyrrole dicarboxylic acid formed in normal adult metabolism, principally from the heme of red cells, at the rate of 250–300 mg per day.^{1,2} Perhaps the most important aspect of the bilirubin molecular structure, concluded from numerous investigations, is its strong propensity to adopt a ridge-tile shape³ with both carboxylic acid groups firmly engaged in intramolecular hydrogen bonding, each to a dipyrinone.^{3–8} Such a structure (Figure 1) explains many of the chemical properties of the pigment, especially its lipophilicity, e.g., soluble in CHCl₃ but insoluble in CH₃OH.⁹ It also helps to understand why bilirubin is not excreted intact by the liver (in contrast to biliverdin or more polar bilirubin isomers where the propionic acids are displaced from C(8) and C(12), e.g., to C(7) and C(13)).^{10,11} For excretion, a specific glucuronosyl transferase enzyme (UGT1A1) converts one or

both of bilirubin's propionic acids to glucuronide esters in the livers of both humans and rats.^{1,12–14}

Effective intramolecular hydrogen bonding between the bilirubin dipyrinones and its carboxylic acid groups requires that the propionic acids (i) stem from C(8) and C(12) and (ii) be capable of orienting their CO₂H termini toward the dipyrinones.^{3,4} Mesobilirubin-XIII_α (Figure 2) has these essential components and orientation, and its most stable conformation is the intramolecularly hydrogen-bonded ridge-tile (as in Figure 1).⁴ Molecular modeling studies indicate that a bilirubin with propionic acids replaced by acrylic acids with *cis* (but not *trans*) carbon–carbon double bonds should adopt an intramolecularly hydrogen-bonded ridge tile conformation. Bilirubins with *ortho* benzoic acid groups replacing propionic acids have their CO₂H groups locked more firmly into the stereochemistry required for intramolecular hydrogen bonding¹⁵ and are predicted to behave similarly. In contrast, the *meta* (**1m**) and *para* (**1p**) regioisomers have longer carbon chain paths connecting C(8)/C(12) to the CO₂H groups, longer carbon chain paths that have their counterparts in (i) the lipophilic rubin with butyric acids replacing propionic, and (ii) in the more polar pentanoic acid rubin.¹⁶ Unlike butyric acid and pentanoic acid rubins, the carbon chain paths of **1m** and **1p** are very inflexible and no more flexible than that of **1o**. In the following we describe the syntheses of **1o**, **1m**, and **1p** and compare their polarity and spectroscopic properties and stereochemistry.

(1) Chowdhury, J. R.; Wolkoff, A. W.; Chowdhury, N. R.; Arias, I. M. Hereditary Jaundice and Disorders of Bilirubin Metabolism. In *The Metabolic and Molecular Bases of Inherited Disease*; Scriver, C. R., Beaudet, A. L., Sly, W. S., Valle, D., Eds.; McGraw-Hill: New York, 2001; Vol. 2, pp 3063–3101.

(2) McDonagh, A. F. Bile Pigments: Bilatrienes and 5, 15-Biladienes. In *The Porphyrins*; Dolphin, D., Ed.; Academic Press: New York, 1979; Vol. 6, pp 293–491.

(3) Bonnett, R.; Davies, J. E.; Hursthouse, M. B.; Sheldrick, G. M. *Proc. R. Soc. London, Ser. B* **1978**, *202*, 249–268.

(4) Person, R. V.; Peterson, B. R.; Lightner, D. A. *J. Am. Chem. Soc.* **1994**, *116*, 42–59.

(5) For leading references, see Sheldrick, W. S. *Isr. J. Chem.* **1983**, *23*, 155–166.

(6) Dörner, T.; Knipp, B.; Lightner, D. A. *Tetrahedron* **1997**, *53*, 2697–2716.

(7) For leading references, see: Kaplan, D.; Navon, G. *Isr. J. Chem.* **1983**, *23*, 177–186.

(8) Navon, G.; Frank, S.; Kaplan, D. *J. Chem. Soc., Perkin Trans. 2* **1984**, 1145–1149.

(9) Lightner, D. A.; McDonagh, A. F. *Acc. Chem. Res.* **1984**, *17*, 417–424.

(10) McDonagh, A. F.; Lightner, D. A. The Importance of Molecular Structure in Bilirubin Metabolism and Excretion. In *Hepatic Metabolism and Disposition of Endo and Xenobiotics*; Bock, K. W., Gerok, W., Matern, S., Eds.; Falk Symposium No. 57; Kluwer: Dordrecht, The Netherlands, 1991, Chapter 5, 47–59.

(11) Ramonas, L. M.; McDonagh, A. F.; Palma, L. A. *J. Pharmacol. Methods* **1981**, *5*, 149–164.

(12) Bosma, P. J.; Seppen, J.; Goldhoorn, B.; Bakker, C.; Oude Elferink, R. P.; Chowdhury, J. R.; Chowdhury, N. R.; Jansen, P. L. *J. Biol. Chem.* **1994**, *269*, 17960–17964.

(13) Coffman, B. L.; Green, M. D.; King, C. D.; Tephly, T. R. *Mol. Pharmacol.* **1995**, *47*, 1101–1105.

(14) Owens, I. S.; Ritter, J. K.; Yeatman, M. T.; Chen, F. *J. Pharmacokinetic. Biopharm.* **1996**, *24*, 491–508.

(15) Boiadjev, S. E.; Lightner, D. A. *Tetrahedron* **2002**, *58*, 7411–7421.

(16) (a) Lightner, D. A.; McDonagh, A. F. *J. Perinatol.* **2001**, *21*, S13–S16. (b) Shrout, D. P.; Puzicha, G.; Lightner, D. A. *Synthesis* **1992**, 328–332.

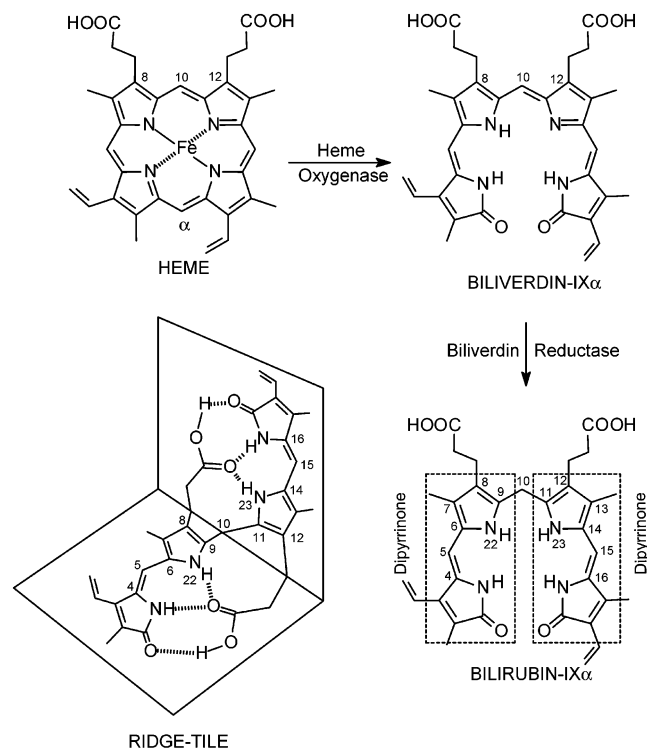


FIGURE 1. Enzymic conversion of heme to biliverdin and biliverdin to bilirubin. The most stable (ridge-tile) conformation of bilirubin (lower left) is one of many possible conformations that arise by rotation of the dipyrinones about C(10) and the only conformation where nonbonded intramolecular steric interactions are minimized and where both carboxylic acid groups engage in intramolecular hydrogen bonding to the opposing dipyrinones. The ridge-tile conformation is defined by torsion angles about both C(10) C–C single bonds [$\phi_1 = \text{N}(22)\text{--C}(9)\text{--C}(10)\text{--C}(11)\text{--N}(23)$], the C(5)–C(6) single bond [$\theta_1 = \text{C}(4)\text{--C}(5)\text{--C}(6)\text{--N}(22)$] and the C(14)–C(15) single bond [$\theta_2 = \text{N}(23)\text{--C}(14)\text{--C}(15)\text{--C}(16)$], where $\phi_1 = \phi_2 = -60^\circ$ and $\theta_1 = \theta_2 = 0^\circ$. (In the porphyrin-like shape of biliverdin (right), $\phi_1 = \phi_2 = 0^\circ$.)

Results and Discussion

Syntheses. As in other reported syntheses of rubins and verdins, the tetrapyrroles of this study were obtained following oxidative coupling of dipyrinones using chloranil in dichloromethane and formic acid at 40°C (Scheme 1). Thus, **5o** gave verdin ester **3o**, **5m** gave **3m**, and **5p** gave **3p**, all in good yield. The isobutyl ester was chosen for the *para* series to overcome the extreme insolubility of the dipyrinone methyl ester and to facilitate handling of the rubin ester (**2p**). Reduction of the verdin esters using sodium borohydride converted the deep blue verdin color to the bright yellow rubin color, and the surprisingly stable rubin ester benzoic acids were isolated in 91–93% yield following radial chromatography and crystallization. Saponification of rubin esters (**2**) afforded the benzoic acid rubins (**1**), of which **1m** and **1p** were decidedly more polar than **1o**.

Biaryls containing conjoined sterically hindered 3-pyrrolyl and *meta* or *para* carboxy (or carboalkoxy) phenyl moieties are not known. In principle their syntheses might be achieved by a classical Fischer–Knorr pyrrole ring closure¹⁷ using the appropriate 3-arylpentane-2,4-dione. Although arylation of the sodium salt of pentane-

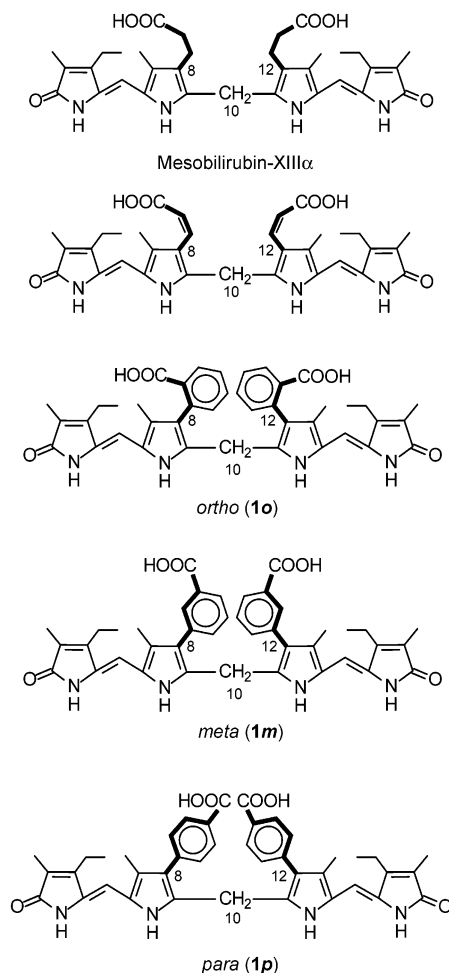


FIGURE 2. Mesobilirubin-XIII α and its analogue with an alkanolic acid chain-stiffening double bond, and the regioisomeric benzoic acid rubins with carboxyphenyl groups replacing propionic acids.

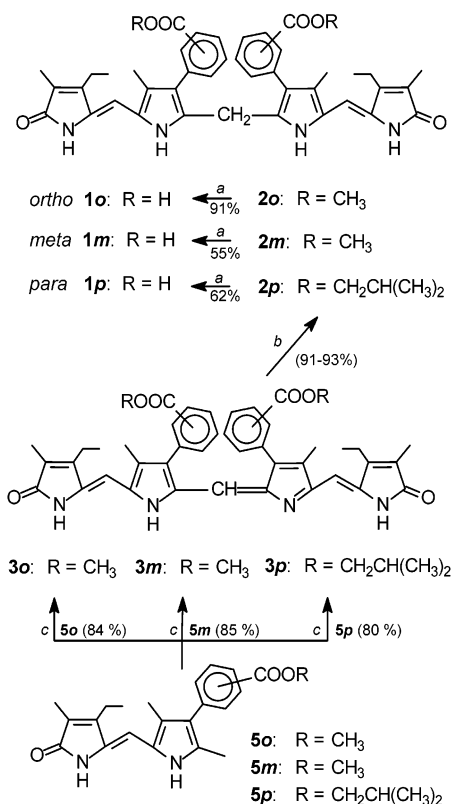
2,4-dione with sodium *o*-bromobenzoate has been reported,¹⁸ and the product successfully used in pyrrole synthesis,¹⁵ the *m*- and *p*-bromobenzoates do not react in the same manner.^{18a} An alternative approach to pyrrole ring formation involved base-catalyzed Barton–Zard reaction of α -isocyano esters with nitroalkenes (or β -acetoxy nitroalkanes as convenient surrogates).¹⁹ The initial stages of such an approach, condensing methyl *m*- or *p*-formylbenzoates and nitroethane, followed by condensation with benzyl isocyanoacetate were explored. This route leads to 9-benzoyloxycarbonyl dipyrinones²⁰ and thus necessitates further elaboration of the resulting 9-ester group in order to convert the dipyrinone to a linear tetrapyrrole. In light of this perceived encumbrance, we were more inclined toward a Suzuki coupling reaction²¹ on a preformed pyrrole nucleus.

(17) Fischer, H.; Orth, H. *Die Chemie des Pyrroles*; Akademische Verlag GmbH: Leipzig, 1934; Vol. I.

(18) (a) Bacon, R. G. R.; Murray, J. C. F. *J. Chem. Soc., Perkin Trans. 1* **1975**, 1267–1272. (b) Aalten, H. L.; van Koten, G.; Vrieze, K.; van der Kerk-van Hoof, A. *Recl. Trav. Chim. Pays-Bas* **1990**, 109, 46–54.

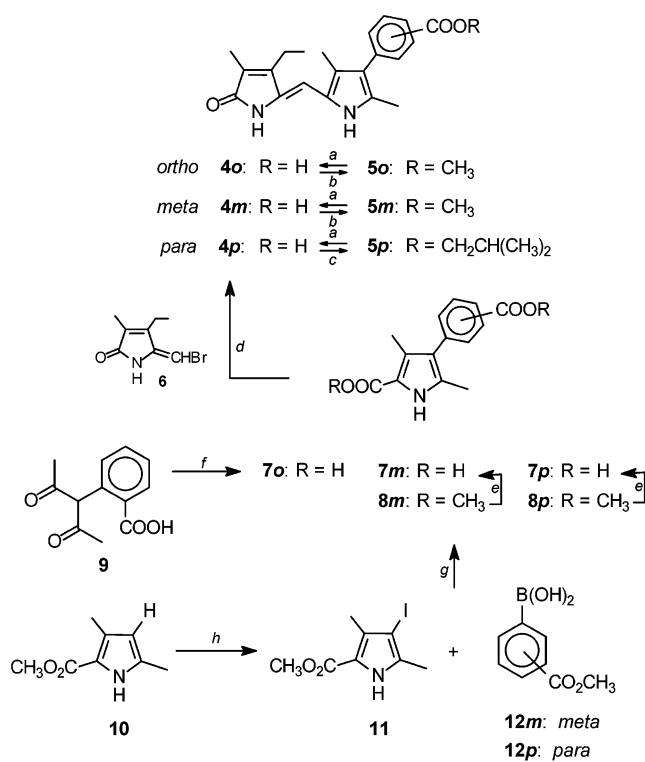
(19) Barton, D. H. R.; Kervagoret, J.; Zard, S. Z. *Tetrahedron* **1990**, 46, 7587–7598.

(20) (a) Kinoshita, H.; Ngwe, H.; Kohori, K.; Inomata, K. *Chem. Lett.* **1993**, 1441–1442. (b) Kohori, K.; Hashimoto, M.; Kinoshita, H.; Inomata, K. *Bull. Chem. Soc. Jpn.* **1994**, 67, 3088–3093.

SCHEME 1^a

^a Reagents and conditions: (a) NaOH/EtOH–H₂O, then HCl; (b) NaBH₄/CH₃OH–CHCl₃; (c) chloranil/HCO₂H, Δ .

Suzuki coupling of a β -bromopyrrole with phenylboronic acid has been reported,²² but carbo(alkoxy)-substituted boronic acids were not known to be participants in the Suzuki coupling reaction with pyrroles. The precursors, *m*-(methoxycarbonyl)phenyl boronic acid (**12m**)²³ and its *p*-isomer (**12p**),²⁴ were prepared inexpensively by a combination of literature methods. Commercially available *m*- or *p*-bromotoluene easily formed Grignard reagents, which were reacted (inverse addition at –78 °C) with trimethyl borate. During the acidic workup, the borate ester hydrolyzed to furnish the corresponding tolyboronic acids. Permanganate oxidation of the methyl group to a carboxylic acid was followed by acid-catalyzed esterification to afford **12m** and **12p** (Scheme 2). Methyl 3,5-dimethyl-1*H*-pyrrole-2-carboxylate (**10**)²⁵ was iodinated at the β -position using KI/H₂O₂²⁶ to give almost quantitatively the iodopyrrole **11**. Reaction of **11** with

SCHEME 2^a

^a Reagents and conditions: (a) NaOH/EtOH–H₂O, Δ , then HCl; (b) CH₂N₂; (c) (CH₃)₂CHCH₂I/Cs₂CO₃/DMF; (d) CH₃OH, Δ ; (e) NaOH/EtOH–H₂O, Δ , then HNO₃/aq. NaNO₃; (f) HON=C(CO₂Et)₂/Zn/HOAc/NaOAc, Δ ; (g) Pd(PPh₃)₄, DMF, aq. Na₂CO₃, Δ ; (h) KI, H₂O₂, EtOH–H₂O, Δ .

boronic acid **12** for 16–18 h at elevated temperature, following the conditions suggested for phenylboronic acid,²² yielded only 15–20% of the desired biaryl **8** after tedious chromatographic separation. Numerous optimization efforts, including changing the solvent and base, and using conditions for hindered substrates^{21b} (38% yield) led to little or no improvement. Examining the composition of the reaction mixture with time revealed that the coupling is essentially complete within a very short time, 15–25 min at 100–105 °C when 4 mol % of Pd(PPh₃)₄²⁷ catalyst and aqueous Na₂CO₃ were used in oxygen-free dimethylformamide solvent. Under these conditions both **12m** and **12p** reacted similarly with iodopyrrole **11** to afford consistent 75–78% yields of arylpyrroles **8m** and **8p**, respectively. The β -bromopyrrole analogue of **11** showed an identical reactivity in a Suzuki reaction under the same conditions.

Standard saponification of the dimethyl esters **8m** or **8p** to their diacids (**7m** and **7p**, respectively), followed by condensation with 5-bromomethylene-4-ethyl-3-methyl-2-oxo-1*H*-pyrrole (**6**),²⁸ afforded crude yellow dipyrrole acids **4m** and **4p**, respectively (Scheme 2). Curiously, when this type of condensation is performed using pyrrole diacids with an alkanolic side chain,^{28,29} the dipyrrole acids formed are esterified in the alkanolic acid side chain from reaction with methanol solvent under

(21) (a) Miyaura, N.; Suzuki, A. *Chem. Rev.* **1995**, *95*, 2457–2483. (b) Watanabe, T.; Miyaura, N.; Suzuki, A. *Synlett* **1992**, 207–210 (for hindered substrates). (c) Suzuki, A. *J. Organomet. Chem.* **1999**, *576*, 147–168.

(22) Chang, C. K.; Bag, N. *J. Org. Chem.* **1995**, *60*, 7030–7032.

(23) (a) Suenaga, H.; Nakashima, K.; Mikami, M.; Yamamoto, H.; James, T. D.; Samankumara Sandanayake, K. R. A.; Shinkai, S. *Recl. Trav. Chim. Pays-Bas* **1996**, *115*, 44–48. (b) Haino, T.; Matsumura, K.; Harano, T.; Yamada, K.; Saijyo, Y.; Fukazawa, Y. *Tetrahedron* **1998**, *54*, 12185–12196.

(24) (a) Matsubara, H.; Seto, K.; Tahara, T.; Takahashi, S. *Bull. Chem. Soc. Jpn.* **1989**, *62*, 3896–3901. (b) Hylarides, M. D.; Wilbur, D. S.; Hadley, S. W.; Fritzberg, A. R. *J. Organomet. Chem.* **1989**, *367*, 259–265.

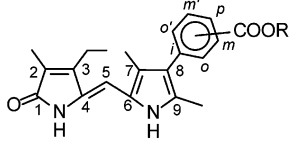
(25) Boiadjev, S. E.; Lightner, D. A. *Tetrahedron: Asymmetry* **2002**, *13*, 1721–1732.

(26) Treibs, A.; Kolm, H. G. *Liebigs Ann. Chem.* **1958**, *614*, 176–198.

(27) Coulson, D. R. *Inorg. Synth.* **1990**, *28*, 107–109.

(28) Shrout, D. P.; Lightner, D. A. *Synthesis* **1990**, 1062–1065.

(29) Puzicha, G.; Shrout, D. P.; Lightner, D. A. *J. Heterocycl. Chem.* **1990**, *27*, 2117–2123.

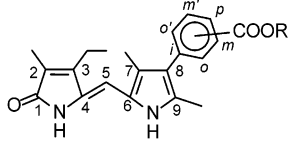
TABLE 1. Comparison of ^{13}C NMR Spectral Assignments of Carboxyphenyl-xanthobilirubic Acids 4 and Their Esters 5^a


position	acids			esters		
	<i>ortho</i> (4o)	<i>meta</i> (4m)	<i>para</i> (4p)	<i>ortho</i> (5o)	<i>meta</i> (5m)	<i>para</i> (5p)
1-CO	172.0	172.1	172.0	172.0	172.0	172.0
2	122.4	122.6	122.7	122.0	122.6	122.8
2-CH ₃	8.1	8.1	8.1	8.1	8.1	8.1
3	147.2	147.3	147.3	147.2	147.3	147.3
3-CH ₂ CH ₃	17.2	17.2	17.2	17.1	17.2	17.1
3-CH ₂ CH ₃	14.9	14.8	14.8	14.8	14.8	14.8
4	127.7	128.57	127.7	127.9	128.6	126.7
5	97.6	97.3	97.2	97.5	97.2	97.1
6	122.2	121.6	121.5	121.8	121.4	121.4
7	122.8	123.4	123.5	123.0	123.4	123.5
7-CH ₃	10.0	10.1	10.2	9.8	10.1	10.2
8	121.9	120.7	120.7	121.8	120.7	120.7
<i>i</i> -	134.9	135.8	140.3	135.3	136.0	140.8
<i>o</i> -	133.9	128.56	129.2	131.9	128.8	129.1
<i>o</i> -	129.0	129.9	129.2	129.2	129.71	129.1
<i>m</i> -	130.4	129.6	129.3	131.2	129.6	129.3
<i>m</i> '-	132.1	126.5	129.3	132.3	126.3	129.3
<i>p</i> -	126.4	133.7	128.7	126.5	134.1	128.8
CO ₂ R	169.5	167.4	167.3	168.0	166.3	165.7
-OCH ₃				51.9	52.2	
-OCH ₂ CH(CH ₃) ₂						70.2
-OCH ₂ CH(CH ₃) ₂						27.4
-OCH ₂ CH(CH ₃) ₂						18.9
9	129.5	130.8	130.0	129.4	129.67	130.1
9-CH ₃	11.6	11.8	12.0	11.5	11.8	11.9

^a Acquired in 2×10^{-2} M solutions in (CD₃)₂SO solvent at 25 °C.

acidic reaction conditions. In contrast, only a partial esterification (<10%) occurred in the syntheses of **4m** and **4p**, consistent with what was detected earlier in the preparation of **4o**.¹⁵ Possibly the dipyrinones **4** are much less soluble in methanol than their counterparts with alkanolic acid chains and precipitate soon after their formation, thereby slowing any subsequent esterification. The *m*-methyl ester **5m** was prepared in 75% yield from crude acid **4m** by esterification with an excess of diazomethane in ether followed by purification using chromatography. Similar treatment of the crude *p*-acid **4p** gave a surprisingly insoluble methyl ester that was not suitable for purification by chromatography. Therefore, an S_N2 esterification process from reaction of isobutyl iodide with the cesium carboxylate salt³⁰ of **4p** was followed. This reaction afforded a 58% yield of isobutyl ester **5p** (based on the amount of starting **8p**), which showed favorable solubility and was amenable to chromatographic purification.

The purified bright yellow esters (**5**) were saponified quantitatively with aqueous sodium hydroxide in a homogeneous mixture with ethanol. The precipitated acids (**4**) are nearly insoluble in nonpolar solvents and only partially soluble in methanol. They are, however,

TABLE 2. Comparison of ^1H NMR Spectral Assignments of Carboxyphenyl-xanthobilirubic Acids 4 and Their Esters 5^a


position	acids (δ)			esters (δ)		
	<i>ortho</i> (4o)	<i>meta</i> (4m)	<i>para</i> (4p)	<i>ortho</i> (5o)	<i>meta</i> (5m)	<i>para</i> (5p)
pyrrole NH	10.53	10.66	10.68	10.54	10.66	10.69
lactam NH	9.84	9.84	9.84	9.83	9.84	9.84
2-CH ₃	1.79	1.79	1.79	1.79	1.79	1.79
3-CH ₂ CH ₃	2.51 ^b	2.52 ^b	2.52 ^b	2.51 ^b	2.52 ^b	2.52 ^p
3-CH ₂ CH ₃	1.09 ^c	1.10 ^c	1.10 ^c	1.09 ^c	1.10 ^c	1.10 ^q
5-CH=	5.96	6.00	6.00	5.97	6.00	6.00
7-CH ₃	1.90	2.07	2.09	1.87	2.06	2.09
<i>o</i> -H		7.79 ^f	7.36 ⁱ		7.79 ⁿ	7.40 ^r
<i>o</i> '-H	7.18 ^d	7.49 ^g	7.36 ⁱ	7.22 ^j	7.52 ^o	7.40 ^r
<i>m</i> -H	7.73 ^d		7.95 ⁱ	7.75 ^k		7.98 ^r
<i>m</i> '-H	7.50 ^e	7.52 ^e	7.95 ⁱ	7.56 ^l	7.55 ^e	7.98 ^r
<i>p</i> -H	7.36 ^e	7.82 ^h		7.40 ^m	7.83 ^o	
-OCH ₃				3.64	3.85	
-OCH ₂ CH(CH ₃) ₂						4.07 ^s
-OCH ₂ CH(CH ₃) ₂						2.02 ⁿ
-OCH ₂ CH(CH ₃) ₂						0.98 ^t
-CO ₂ H	12.57	12.94	12.79			
9-CH ₃	2.06	2.25	2.27	2.04	2.24	2.27

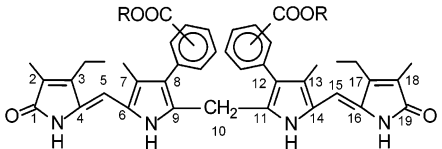
^a Acquired in 2×10^{-2} M solutions in (CD₃)₂SO solvent at 25 °C. ^b q, $J = 7.6$ Hz. ^c t, $J = 7.6$ Hz. ^d d, $^3J = 7.6$ Hz. ^e dd, $^3J = 7.6$, $^4J = 1.5$, $^5J = 1.6$ Hz. ^f br. dd, $^4J = 1.5$, $^5J = 1.6$ Hz. ^g ddd, $^3J = 7.6$, $^4J = 1.5$, $^5J = 1.6$ Hz. ^h ddd, $^3J = 7.6$, $^4J = 1.6$, $^5J = 1.6$ Hz. ⁱ br. d, $^3J = 8.2$ Hz. ^j dd, $^3J = 7.7$, $^4J = 0.9$ Hz. ^k dd, $^3J = 7.7$, $^4J = 1.1$ Hz. ^l ddd, $^3J = 7.7$, $^4J = 1.1$ Hz. ^m ddd, $^3J = 7.7$, $^4J = 0.9$ Hz. ⁿ m. ^o br. d, $^3J = 7.6$ Hz. ^p q, $J = 7.7$ Hz. ^q t, $J = 7.7$ Hz. ^r br. d, $J = 8.3$ Hz. ^s d, $J = 6.4$ Hz. ^t d, $J = 6.7$ Hz.

soluble in DMSO. The corresponding sodium or ammonium salts are rather soluble in both methanol and water.

The synthesis of the *ortho* compounds has been reported previously¹⁵ and for purposes of comparison is outlined briefly here and in Scheme 2. At the time the work was initiated, pyrroles substituted with β *o*-carboethoxyphenyl, *o*-carbomethoxyphenyl, or *o*-carboxyphenyl groups were unknown. For purposes of Suzuki coupling to make the diester of **7**, although *m*- and *p*-carboxy (or carboalkoxy) phenylboronic acids had been described in the literature, the *o*-isomer had not. We therefore decided to pursue a more classical Fischer–Knorr synthesis from 3-(*o*-carboxyphenyl)-pentane-2,4-dione. 3-(*o*-Carboxyphenyl)-pentane-2,4-dione (**9**) was prepared in high yield by reaction of sodium *o*-bromobenzoate with the sodium salt of pentane-2,4-dione.¹⁸ The resulting acid (**9**) under the same Fischer–Knorr pyrrole-forming condensation conditions afforded a 65% isolated yield of pyrrole α -ester of acid **7o**, which was saponified to **7o** and condensed smoothly with **6** to afford **4o**. Attempted oxidative coupling of dipyrinone acid **4o** gave no verdin, apparently because of interference (by proton transfer) from the free CO₂H group; however, oxidative coupling of dipyrinone ester **5o** gave a mixture of verdins **2o** in 91% yield.

Molecular Structure. The constitutional structures of **4** and **5** follow from the methods of synthesis and from

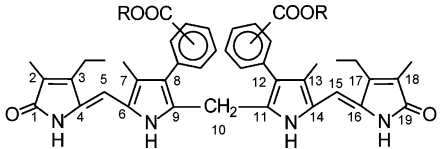
(30) (a) Dijkstra, G.; Kruijzinga, W. H.; Kellogg, R. M. *J. Org. Chem.* **1987**, *52*, 4230–4234. (b) Kunz, H.; Lerchen, H.-G. *Tetrahedron Lett.* **1987**, *28*, 1873–1876.

TABLE 3. Comparison of ^{13}C NMR Spectral Assignments of Carboxyphenyl-mesobilirubins **1** and **2**^a


position	R = H			R = alkyl		
	<i>ortho</i> (1o) ^b	<i>meta</i> (1m)	<i>para</i> (1p)	<i>ortho</i> (2o) ^c	<i>meta</i> (2m)	<i>para</i> (2p)
COOR	168.9 169.1	167.3	167.2	167.4 167.5	166.1	165.6
1,19-CONH	172.0 172.0	172.1	172.1	172.0 172.0	172.0	172.1
2,18	123.1 123.1	123.6	123.8	123.1 123.2	123.5	123.8
2,18-CH ₃	8.1 (br.)	8.1	8.1	8.07 8.08	8.1	8.1
3,17	147.1 147.2	147.2	147.2	147.1 147.2	147.2	147.1
3,17-CH ₂ CH ₃	17.17 17.18	17.2	17.2	17.15 17.16	17.2	17.2
3,17-CH ₂ CH ₃	14.9	14.8	14.8	14.9	14.8	14.7
4,16	128.2 128.4	129.2	129.6	128.3 128.5	129.0	129.6
5,15	97.8 97.9	97.5	97.3	97.7 (br.)	97.2	97.2
6,14	122.0 122.1	120.8	120.6	121.8 121.9	120.9	120.6
7,13	122.1 122.2	122.4	122.4	122.0 122.1	122.2	122.2
7,13-CH ₃	9.86 9.89	9.9	10.1	9.68 9.70	9.8	10.0
8, 12	122.6 122.7	122.9	123.2	122.2 122.3	122.8	123.1
<i>i, i</i>	134.8 134.9	135.2	139.7	135.2 135.3	135.4	140.1
<i>o, o</i>	132.9 133.0	130.1	128.8	131.2 131.4	129.9	128.5
<i>o', o'</i>	128.8 129.0	133.6	128.8	129.0 129.1	133.9	128.5
<i>m, m</i>	130.2 130.4	130.3	129.2	130.7 131.0	129.6	129.3
<i>m', m'</i>	132.0 132.1	127.8	129.2	132.2 (br.)	127.9	129.3
<i>p, p</i>	126.18 126.24	126.4	127.7	126.2 126.4	126.2	126.8
R = CH ₃				51.68 51.72	51.9	
R = CH ₂ CH(CH ₃) ₂						70.1
R = CH ₂ CH(CH ₃) ₂						27.4
R = CH ₂ CH(CH ₃) ₂						18.9
9,11	130.1 130.5	129.6	129.8	129.9 130.3	129.1	130.0
10	23.9 24.2	23.9	24.1	23.8 24.0	24.1	24.1

^a Acquired in 2×10^{-2} M solutions in $(\text{CD}_3)_2\text{SO}$ solvent at 25 °C. ^b Italicized signals dominate 65:35. ^c Ratio ~1:1.

their ^{13}C NMR spectra. Thus, the ^{13}C resonances assignable to the dipyrinone skeleton of the *ortho*, *meta*, and *para* isomers of dipyrinones **4** and **5** (Table 1) all correlate nicely, with only slight differences in chemical shifts. The main differences, as expected, lie with resonances coming from the benzoic acid moiety, due to the differing substitution patterns of the aromatic ring. A similarly good correlation is found in their ^1H NMR spectra (Table 2), with the main distinguishing features coming from the benzoic acid resonances. The more shielded C(7) and C(9) methyls of **4o** or **5o** (relative to those in

TABLE 4. Comparison of ^1H NMR Spectral Assignments of Carboxyphenyl-mesobilirubins **1** and **2**^a


position	R = H (δ)			R = alkyl (δ)		
	<i>ortho</i> (1o) ^b	<i>meta</i> (1m)	<i>para</i> (1p)	<i>ortho</i> (2o) ^c	<i>meta</i> (2m)	<i>para</i> (2p)
2,18-CH ₃	1.78 1.79	1.79	1.79	1.78 1.79	1.79	1.79
3,17-CH ₂ CH ₃	2.50 ^d 2.51 ^d	2.50 ^d	2.50 ^k	2.51 ^d 2.52 ^d	2.50 ^d	2.50 ^d
3,17-CH ₂ CH ₃	1.09 ^e 1.10 ^e	1.10 ^e	1.09 ^l	1.09 ^e 1.10 ^e	1.10 ^e	1.09 ^e
5,15-CH=	5.91 5.93	5.91	5.93	5.91 5.92	5.87	5.92
7,13-CH ₃	1.73 1.77	1.89	1.93	1.71 1.72	1.84	1.92
<i>o, o</i>		7.54 ^h	7.06 ^m		7.46 ^s	7.08 ^w
<i>o', o'</i>	6.63 ^f 6.82 ^f	7.16 ^h	7.06 ^m	6.72 ⁿ 6.78 ^o	7.15 ^t	7.08 ^w
<i>m, m</i>	7.66 ^g 7.70 ^g		7.75 ^m	7.67 ^p 7.69 ^q		7.75 ^w
<i>m', m'</i>	7.23– 7.31 ^h	7.27 ^h	7.75 ^m	7.26– 7.33 ^h	7.29 ^u	7.75 ^w
<i>p, p</i>	7.23– 7.31 ^h	7.68 ^h		7.26– 7.33 ^h	7.66 ^v	
COOH	12.32	12.73	12.66			
CO ₂ CH ₃				3.51 3.54	3.75	
CO ₂ CH ₂ – CH(CH ₃) ₂						4.01 ^x
CO ₂ CH ₂ – CH(CH ₃) ₂						1.99 ^h
CO ₂ CH ₂ – CH(CH ₃) ₂						0.96 ^y
10-CH ₂	3.57; 3.78 ⁱ	4.03	4.06	3.56, 3.75 ⁱ	4.04	4.08
21,24- lactam NH	3.74 ^j 9.71	9.72	9.76	3.67 ^j 9.72	9.68	9.72
22,23- pyrrole NH	9.77 10.08	10.39	10.46	9.79 10.13	10.40	10.47

^a Acquired in 2×10^{-2} M solutions in $(\text{CD}_3)_2\text{SO}$ solvent at 25 °C. ^b Italicized signals dominate 65:35. ^c Ratio ~1:1. ^d q, $J = 7.6$ Hz. ^e t, $J = 7.6$ Hz. ^f dd, $^3J = 7.0$, $^4J = 1.0$ Hz. ^g dd, $^3J = 7.5$, $^4J = 1.4$ Hz. ^h m. ⁱ AB, $^2J = 16.8$ Hz. ^j s. ^k q, $J = 7.5$ Hz. ^l t, $J = 7.5$ Hz. ^m d, $J = 8.0$ Hz. ⁿ dd, $^3J = 7.5$, $^4J = 1.1$ Hz. ^o dd, $^3J = 7.6$, $^4J = 1.1$ Hz. ^p dd, $^3J = 7.5$, $^4J = 1.5$ Hz. ^q dd, $^3J = 7.7$, $^4J = 1.5$ Hz. ^r ddd, $^3J = 7.5$; 7.5 , $^4J = 1.5$ Hz. ^s dd, $^4J = 1.7$; 1.6 Hz. ^t ddd, $^3J = 7.8$, $^4J = 1.7$; 1.6 Hz. ^u dd, $^3J = 7.8$; 7.7 Hz. ^v ddd, $^3J = 7.7$; $^4J = 1.7$; 1.6 Hz. ^w d, $J = 8.1$ Hz. ^x d, $J = 6.5$ Hz. ^y d, $J = 6.7$ Hz.

4m, **4p**, **5m**, and **5p**) may be attributed to the magnetic anisotropy of the benzene ring, which is more constrained to be perpendicular to the attached pyrrole ring in order to minimize nonbonded steric interaction between sets of three “ortho” groups ($2 \times \text{CH}_3 + 1 \times \text{CO}_2\text{H}$ in **4o** and **5o**).

In complete correspondence, the constitutional structures of **1** and **2** follow from their syntheses (from **4** and **5**) and from their ^{13}C NMR spectra (Table 3), which show the expected characteristic carbon resonances for the pyrrolinone and pyrrole units, and their β -substituents. Again the distinctive *ortho*, *meta*, and *para* substitution patterns from the benzoic acid resonances find good correlation with the indicated structures.

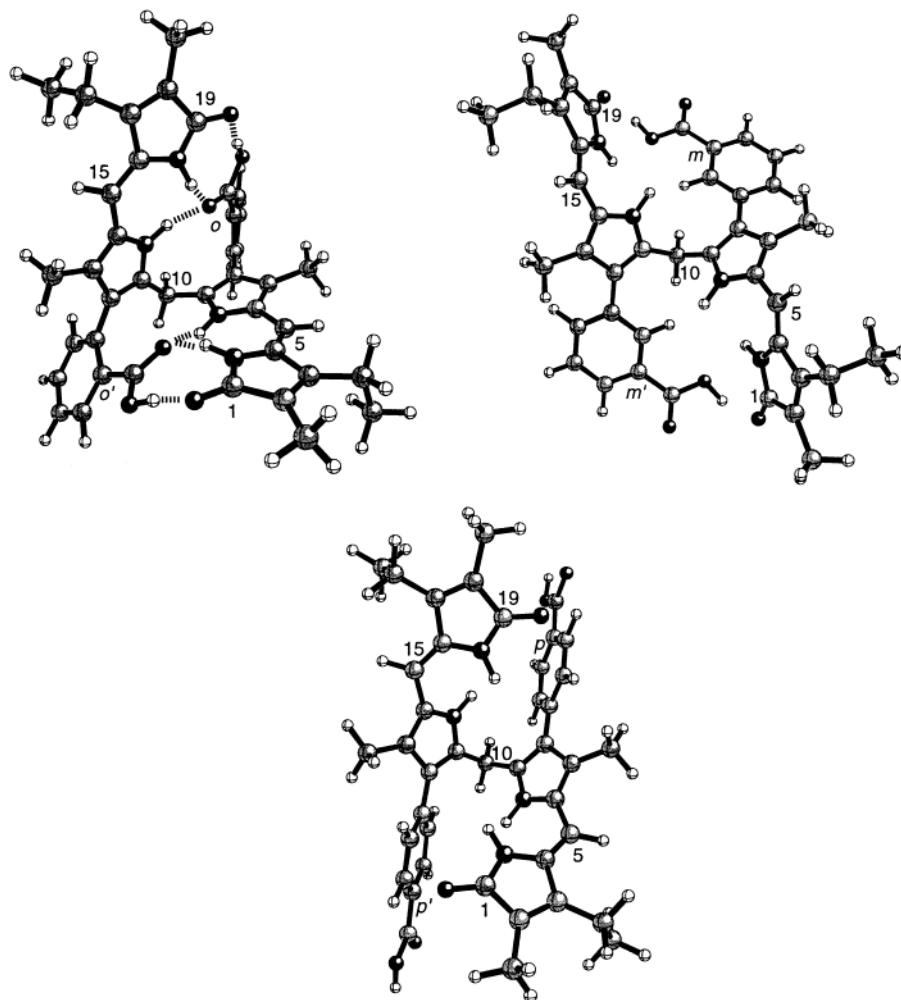


FIGURE 3. Ball and Stick (ref 33) conformational representations of the most stable *P*-helical conformers of **1** with two dipyrinones shaped like a ridge-tile. In **1o** (upper left) considerable conformational stabilization is afforded by intramolecular hydrogen bonding between the dipyrinones and the opposing *o*-carboxyphenyl groups. Such hydrogen bonding (and hence conformational stabilization) is spatially impossible in **1m** (upper right) and **1p** (lower). The shape of each isomer of **1** may be defined by the torsion angles ϕ_1 , ϕ_2 , θ_1 , and θ_2 (see Figure 1), where in **1o**, $\phi_1 \approx \phi_2 \approx 60^\circ$ and $\theta_1 \approx \theta_2 \approx -14^\circ$; in **1m**, $\phi_1 \approx \phi_2 \approx 70^\circ$ and $\theta_1 \approx \theta_2 \approx 45^\circ$; and in **1p**, $\phi_1 \approx \phi_2 \approx 80^\circ$ and $\theta_1 \approx \theta_2 \approx -41^\circ$.

Small but perhaps characteristic differences may be found in the chemical shifts of (i) the C(4/16) resonances, which are more shielded by ~ 1 ppm in **1o** and **2o** than in **1m**, **1p**, **2m**, or **2p** and (ii) the C(6/14) resonances, which are more deshielded by ~ 1 ppm in **1o** and **2o** than in **1m**, **2m**, **1p**, or **2p**. As detected previously,¹⁵ the doubled carbon signals in **1o** and **2o** give clear evidence of diastereotopicity (due to restricted rotation about the pyrrole to benzoic acid bond). Similar evidence for atropisomerism is not found in **1m** or **2m**. Consistent with the conclusions from ^{13}C NMR, the ^1H NMR spectra (Table 4) of **1** and **2** show few differences, except for those attending the differing substitution pattern of the benzoic acid rings and the evidence for atropisomerism found in **1o** and **2o**. Again, as in dipyrinones **4** and **5**, the C(7/13)–CH₃ and C(10)–CH₂ resonances of **1o** and **2o** show a greater shielding than in **1m**, **1p**, **2m**, and **2p** because the aromatic rings are more constrained to remain orthogonal to the pyrrole rings in **1o** and **2o**.

Solution Properties. The bilirubin with *o*-benzoic acid groups (**1o**) exhibits considerably different solubility

properties than those of the *meta* (**1m**) and *para* (**1p**). It is soluble in CHCl₃; the latter two are insoluble. It is insoluble in CH₃OH; the latter two are slightly soluble. Its HPLC retention time (26.8 min) using a reverse phase column³¹ is much longer than that of **1m** (8.0 min) or **1p** (7.1 min). In TLC on silica gel using 2% (by vol) CH₃OH in CH₂Cl₂ as eluent: **1o** ($R_f = 0.93$) moved faster than **1m** ($R_f = 0.01$) and **1p** ($R_f = 0.02$). In 8% CH₃OH–CH₂Cl₂: **1o** ($R_f = 1.00$), **1m** ($R_f = 0.08$), and **1p** ($R_f = 0.09$). The data indicate that **1m** and **1p** exhibit very similar polarity and solubility properties, that these isomers are much more polar than **1o**. Among bilirubins, such large differences are in accord with a structural model in which the polar carboxylic acid groups of **1o** are hydrogen-bonded intramolecularly to the dipyrinones, whereas in **1m** and **1p**, such intramolecular hydrogen bonding is absent. No such large differences in solubility

(31) McDonagh, A. F.; Palma, L. A.; Lightner, D. A. *J. Am. Chem. Soc.* **1982**, *104*, 6867–6869.

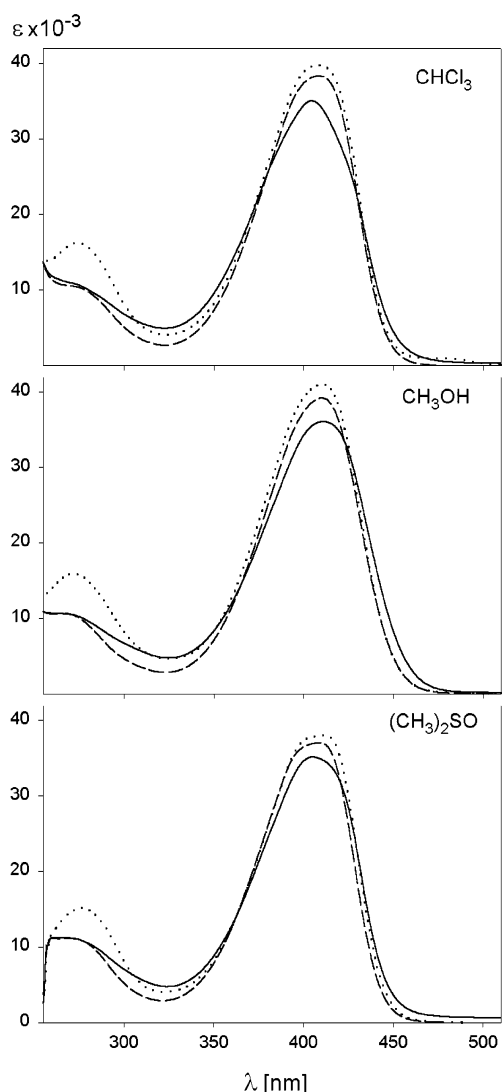


FIGURE 4. Long-wavelength UV-vis absorption curves of the isomeric benzoic-xanthobilirubic acids **4o** (—), **4m** (---), and **4p** (····) in CHCl_3 , CH_3OH , and $(\text{CH}_3)_2\text{SO}$ solvent run at $3.5\text{--}4.0 \times 10^{-5}$ M at 23 °C. The CHCl_3 and CH_3OH solutions contained 2% (by vol) $(\text{CH}_3)_2\text{SO}$.

properties and polarity are evident for the isomeric rubin esters (**2**) or the isomeric verdins (**3**).

Molecular Conformation from Molecular Dynamics Calculations. Substantial evidence from investigations of bilirubin stereochemistry has been marshaled to show that (i) the most stable conformation is shaped like a ridge-tile, with the planes of the two dipyrinones intersecting at an angle of $\sim 100^\circ$ and (ii) considerable conformational stabilization is achieved by intramolecular hydrogen bonding.⁴ The computed (Sybyl)^{32,33} global energy minimum conformations of **1** (Figure 3) all show

(32) Boiadjev, S. E.; Person, R. V.; Puzicha, G.; Knobler, C.; Maverick, E.; Trueblood, K. N.; Lightner, D. A. *J. Am. Chem. Soc.* **1992**, *114*, 10123–10133.

(33) The molecular dynamics calculations used to find the global energy minimum conformations of **1** were run on an SGI Octane workstation using vers. 6.4 of the Sybyl forcefield as described in ref 4. The Ball and Stick drawings were created from the atomic coordinates using Müller and Falk's "Ball and Stock" program for the Macintosh (http://www.orc.uni-linz.ac.at/mueller/ball_stick.html).

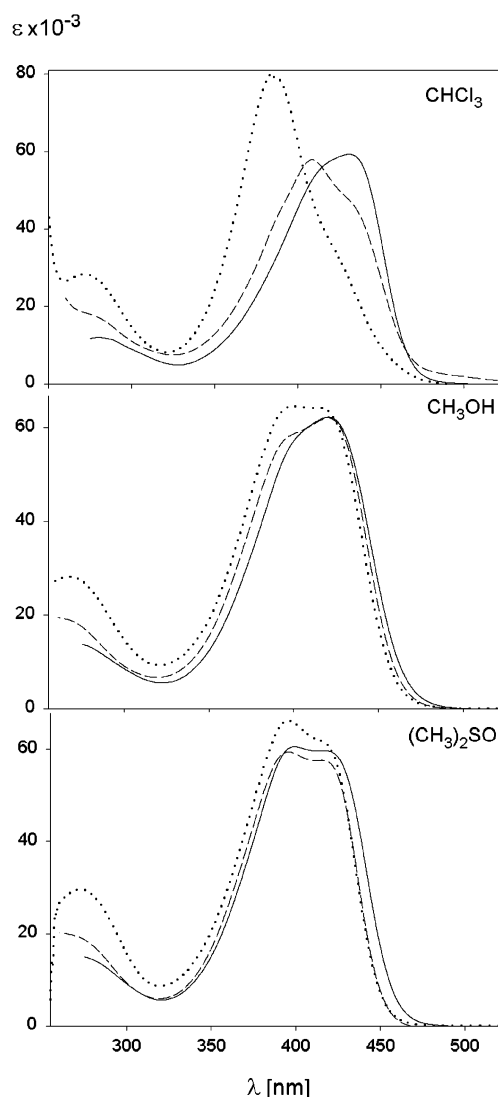


FIGURE 5. Long-wavelength UV-vis absorption curves of benzoic acid rubins **1o** (—), **1m** (---), and **1p** (····) in CHCl_3 , CH_3OH , and $(\text{CH}_3)_2\text{SO}$ solvent run at $1.6\text{--}2.2 \times 10^{-5}$ M at 23 °C. The CHCl_3 and CH_3OH solutions contained 2% (by vol) $(\text{CH}_3)_2\text{SO}$.

the expected folded, ridge-tile structures. They differ only slightly in overall shape, as determined by torsion angles about C(10), C(5)/C(15) (see Figure 1). In **1o**, $\phi_1 \approx \phi_2 \approx 60^\circ$ and $\theta_1 \approx \theta_2 \approx -14^\circ$; in **1m**, $\phi_1 \approx \phi_2 \approx 70^\circ$ and $\theta_1 \approx \theta_2 \approx 45^\circ$; in **1p**, $\phi_1 \approx \phi_2 \approx 80^\circ$ and $\theta_1 \approx \theta_2 \approx -41^\circ$. The conformation of **1o** is greatly stabilized by intramolecular hydrogen bonding; those of **1m** and **1p** arise by minimization of nonbonding steric repulsions. In **1**, the benzoic acid ring is not coplanar with the conjoined pyrrole. As a result of intramolecular hydrogen bonding in **1o**, the twist angle of the phenyl ring is $\sim 75^\circ$, but in **1m** and **1p** it is $142\text{--}148^\circ$. Some weak residual hydrogen bonding between the CO_2H and lactam carbonyl appears in **1m** ($\sim 2.2 \text{ \AA } \text{H} \cdots \text{O}$) but the CO_2H carbonyl to NH hydrogen bonds are absent. While it may be noted that the representations of **1o**, **1m**, and **1p** all belong to the same molecular chirality, the helicity represented is opposite to that shown for bilirubin in Figure 1. In fact the bilirubin and benzoic acid rubins **1** shown all have isoenergetic nonsuperimposable mirror images.

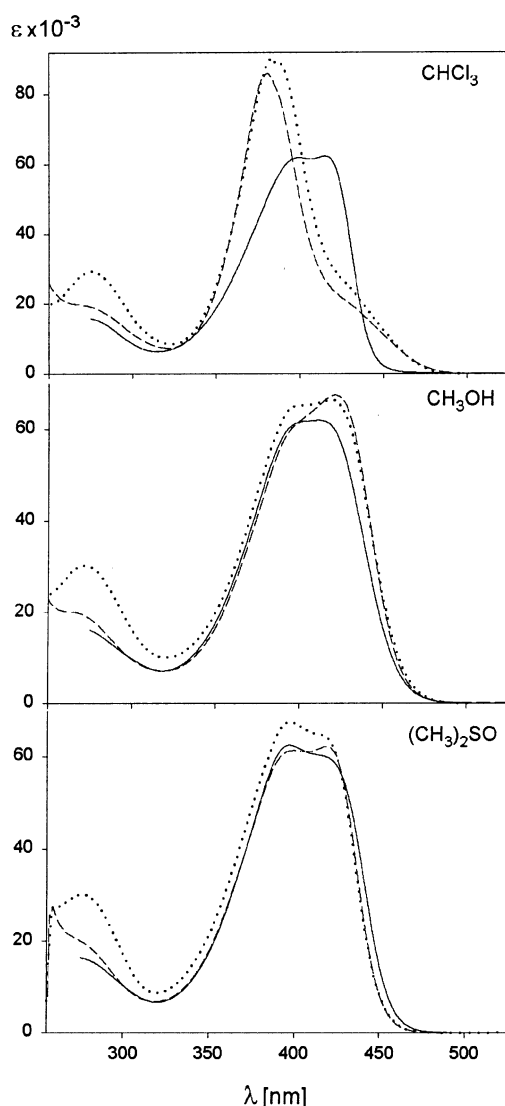


FIGURE 6. Long-wavelength UV-vis absorption curves of benzoic ester rubins **2o** (—), **2m** (---), and **2p** (····) in CHCl_3 , CH_3OH , and $(\text{CH}_3)_2\text{SO}$ solvent run at $1.6\text{--}2.2 \times 10^{-5}$ M at 23 °C. The CH_3OH and $(\text{CH}_3)_2\text{SO}$ solutions contained 2% (by vol) CHCl_3 .

UV-Visible Spectral Analysis. The UV-vis spectral data of **1–5** in a wide range of solvents of different polarity and hydrogen bonding ability are reported in the Experimental Section and illustrated in Figures 4 (for **4**), 5 (for **1**), and 6 (for **2**). The dipyrinones (**4**) show characteristic absorption near 400–410 nm, with ϵ values 35,000–40,000, as is usually seen in other dipyrinone constituents of bilirubin.³⁴ The ϵ values of **1o** are generally lower than those of **1m** and **1p**, due possibly to steric interference of conjugation between the dipyrinone and benzene chromophores. In CHCl_3 , the curves are slightly broader than in CH_3OH or $(\text{CH}_3)_2\text{SO}$, presumably because intermolecularly hydrogen-bonded dimerization is much favored in CHCl_3 .³⁵ The UV-vis spectra of **1** and **2** clearly differ from those of **4**: the curves of Figures 5 and 6 are generally broader than those of **4**, and there is

clear evidence that the long-wavelength absorption consists of two overlapping components. Substantial differences attend the change of solvents from nonpolar CHCl_3 to the more polar solvents. As seen in the UV-vis spectra of other rubins, the band shape consisting of overlapping curves has its origin in exciton coupling^{4,34b,36} and is due to two exciton components originating in an interaction between the electric dipole transition moments in the two proximal dipyrinone chromophores. The exact shape of the composite curve and the transcendence of one component over the other is determined by the relative orientation of the two dipyrinones and can thus provide an insight into conformation of the rubin.⁴ The data are consistent with a conformation where the dipyrinones are oriented at $\sim 100^\circ$ angle (as in Figures 1 and 3), for the ridge-tile conformation for **1o** and **2o**, even for **1m**, **2m**, **1p**, and **2p** in polar solvents such as CH_3OH and $(\text{CH}_3)_2\text{SO}$. In CHCl_3 , which promotes hydrogen bonding, the shape of the UV-vis curves of **1o** and **2o** differ considerably from the others, which show an exaggeration of the shorter wavelength exciton component. Such an exaggeration has been seen previously in the UV-vis spectra of bilirubin dimethyl ester and other rubins incapable of intramolecular hydrogen bonding. It has been attributed to a change in conformation, from ridge-tile to helical, to accommodate effective intermolecular hydrogen bonding in a dimer.³⁵ Such rubins are known to be dimeric in CHCl_3 ; so, it is not surprising that **2m** and **2p** exhibit the UV-vis curves shown in CHCl_3 . It is surprising that **2o** does not, and the data suggest that this ester continues to adopt a ridge-tile shape and would be monomeric in CHCl_3 . The UV-vis data in CHCl_3 for the benzoic acid rubins are consistent with a ridge-tile conformation (Figure 3) in **1o**, and a tendency toward the ridge-tile in **1m**, but very likely an intermolecularly hydrogen-bonded dimer for **1p**.

Induced Circular Dichroism and Conformation.

As observed previously with bilirubin and its analogues, circular dichroism (CD) is induced in the presence of chiral solvating agents.^{37,38} The origin of the CD can be deduced from two observations: (i) bilirubin behaves like a molecular exciton consisting of two dipyrinones interacting by excited-state dipole-dipole coupling, and (ii) the pigment adopts either of two interconverting enantiomeric ridge-tiles, as depicted in Figure 7.⁴ The component dipyrinone chromophores of **1** have strongly allowed long-wavelength electric dipole transition moments (Table 5), making them excellent candidates for induced electric dipole-electric dipole (Figure 7) interac-

(35) (a) Huggins, M. T.; Lightner, D. A. *Monatsh. Chem.* **2001**, *132*, 203–221. (b) Boiadjev, S. E.; Lightner, D. A. *J. Heterocycl. Chem.* **2000**, *37*, 863–870.

(36) Harada, N.; Nakanishi, K. *Circular Dichroic Spectroscopy—Exciton Coupling in Organic Stereochemistry*; University Science Books: Mill Valley, CA, 1983.

(37) Boiadjev, S. E.; Lightner, D. A. *Tetrahedron: Asymmetry* **1999**, *10*, 607–655.

(38) (a) Reisinger, M.; Lightner, D. A. *J. Inclusion Phenom.* **1985**, *3*, 479–486. (b) Lightner, D. A.; An, J. Y.; Pu, Y.-M. *Tetrahedron* **1987**, *43*, 4287–4296. (c) Lightner, D. A.; An, J. Y.; Pu, Y. M. *Arch. Biochem. Biophys.* **1988**, *262*, 543–559. (d) Pu, Y. M.; Lightner, D. A. *Croat. Chem. Acta* **1989**, *62*, 301–324. (e) Gawronski, J. K.; Polonski, T.; Lightner, D. A. *Tetrahedron* **1990**, *46*, 8053–8066. (f) Trull, F. R.; Shrout, D. P.; Lightner, D. A. *Tetrahedron* **1992**, *48*, 8189–8198. (g) Kar, A.; Lightner, D. A. *Tetrahedron* **1998**, *54*, 12671–12690. (h) Brower, J. O.; Lightner, D. A.; McDonagh, A. F. *Tetrahedron* **2000**, *56*, 7869–7883. (i) Brower, J. O.; Lightner, D. A.; McDonagh, A. F. *Tetrahedron* **2001**, *57*, 7813–7827.

(34) (a) Byun, Y. S.; Lightner, D. A. *J. Org. Chem.* **1991**, *56*, 6027–6033. (b) Lightner, D. A.; Gawronski, J. K.; Wijekoon, W. M. D. *J. Am. Chem. Soc.* **1987**, *109*, 6354–6362.

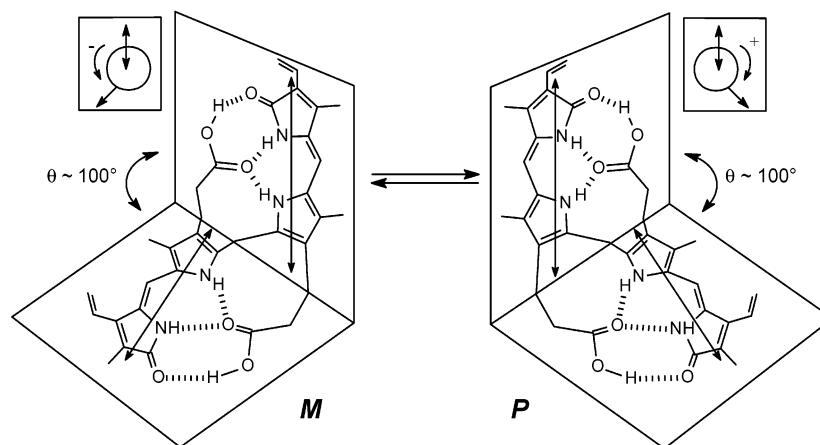


FIGURE 7. Bilirubin 3-D conformational structures shaped like ridge-tiles of left (**M**)- and right (**P**)-handed chirality are isoenergetic, nonsuperimposable mirror images (enantiomers). Dashed lines are hydrogen bonds, and double-headed arrows represent the approximate locations of the dipyrinone long-wavelength electric dipole transition moments. Inset boxes show the relative orientation of the transition dipoles, (+) for **P** helicity and (−) for **M**.

TABLE 5. UV–vis Spectral Data of Carboxyphenyl-mesobilirubins **1** and Their Esters **2**^a

pigment	$\epsilon^{\max} (\lambda^{\max}, \text{nm})$				
	C ₆ H ₆	CHCl ₃	CH ₃ OH	CH ₃ CN	(CH ₃) ₂ SO
<i>ortho</i> (1o) ^b	58,500 (434)	59,300 (431)	62,300 (421)	58,900 (422)	59,700 (416)
	55,800 (419) ^{sh}	57,400 (419) ^{sh}	57,800 (401) ^{sh}		60,600 (399)
<i>meta</i> (1m) ^c	54,400 (420)	47,300 (431) ^{sh}	62,200 (420)	33,900 (417) ^{sh}	57,600 (415)
	64,900 (393)	58,000 (409)	58,200 (397) ^{sh}	69,100 (380)	59,400 (396)
<i>para</i> (1p) ^c	56,600 (418) ^{sh}	36,700 (420) ^{sh}	64,400 (413)	31,900 (418) ^{sh}	61,800 (415) ^{sh}
	72,300 (393)	79,400 (387)	64,600 (400)	83,600 (380)	66,200 (396)
<i>ortho</i> (2o) ^b	53,900 (412) ^{sh}	62,300 (415)	61,900 (411)	39,600 (409) ^{sh}	59,900 (418) ^{sh}
	69,200 (390)	61,800 (399)	61,400 (399) ^{sh}	76,400 (379)	62,500 (397)
<i>meta</i> (2m) ^b	21,200 (429) ^{sh}	20,700 (428) ^{sh}	67,400 (421)	21,200 (421) ^{sh}	62,100 (419)
	85,600 (383)	85,900 (381)	61,100 (398) ^{sh}	88,600 (376)	61,300 (399)
<i>para</i> (2p) ^b	26,600 (428) ^{sh}	25,500 (428) ^{sh}	66,300 (419)	26,200 (419) ^{sh}	65,200 (414) ^{sh}
	93,300 (389)	90,100 (383)	65,200 (401) ^{sh}	94,800 (380)	67,600 (397)

^a Concentration $1.6\text{--}2.2 \times 10^{-5}$ M. ^b All solutions contained 2% v/v of CHCl₃. ^c All solutions contained 2% v/v of (CH₃)₂SO.

tion (exciton coupling). Although one would expect only a weak, monosignate CD associated with a $\pi \rightarrow \pi^*$ excitation from a dipyrinone chromophore perturbed by dissymmetric vicinal action, when two dipyrinone chromophores interact by coupling locally excited $\pi \rightarrow \pi^*$ transitions (electric dipole transition moment coupling),^{4,32,34b,39} one would expect to observe bisignate spectra characteristic of an exciton system.³⁶ The component dipyrinone chromophores of the bichromophoric rubins have strongly allowed long-wavelength electronic transitions ($\epsilon_{410}^{\max} \sim 40,000$) but only a small interchromophoric orbital overlap in the ridge-tile conformation (Figure 1). They are nicely oriented to interact by electrostatic interaction of the local transition moment dipoles, which are polarized along the long axis of each dipyrinone, i.e., resonance splitting. Such intramolecular exciton interaction produces two long-wavelength transitions in the UV–vis spectrum and two corresponding bands in the CD spectrum. One band is higher in energy, and one is lower in energy, with the splitting being dependent on the strength and relative orientation of the

dipyrinone electric dipole transition moments (Figure 7). Observed by UV–vis spectroscopy, the two electronic transitions overlap to give the typically broadened and sometimes split long-wavelength absorption band (Figures 4–6), but in the CD spectra the two exciton transitions are oppositely signed and thus bisignate spectra are typically seen, as predicted by theory.^{4,34b,36}

According to exciton chirality theory,³⁶ the signed order of the bisignate CD Cotton effects may be used to predict the relative orientation of the two electric dipole transition moments, one from each dipyrinone of the rubin. Thus, a negative exciton chirality (long-wavelength negative Cotton effect followed by a positive short wavelength Cotton effect) corresponds to a negative torsion angle between the transition dipoles. On the other hand, a positive exciton chirality (long-wavelength positive Cotton effect followed by a negative short-wavelength Cotton effect) corresponds to a positive torsion angle. Accordingly, the **P**-helical conformer of Figure 3 is predicted to have a positive exciton chirality, and the **M**-helical is predicted to have a negative exciton chirality. In a nonpolar, aprotic solvent (such as chloroform) that promotes hydrogen bonding and association with chiral complexation agents such as quinine, the conformational equilibrium between bilirubin enantiomers can be displaced from 1:1 by adding a chiral recognition agent. This

(39) (a) McDonagh, A. F.; Lightner, D. A.; Reisinger, M.; Palma, L. A. *J. Chem. Soc., Chem. Commun.* **1986**, 249–250. (b) Lightner, D. A.; Wijekoon, W. M. D.; Zhang, M. H. *J. Biol. Chem.* **1988**, *263*, 16669–16676. (c) Pu, Y.-M.; McDonagh, A. F.; Lightner, D. A. *J. Am. Chem. Soc.* **1993**, *115*, 377–380.

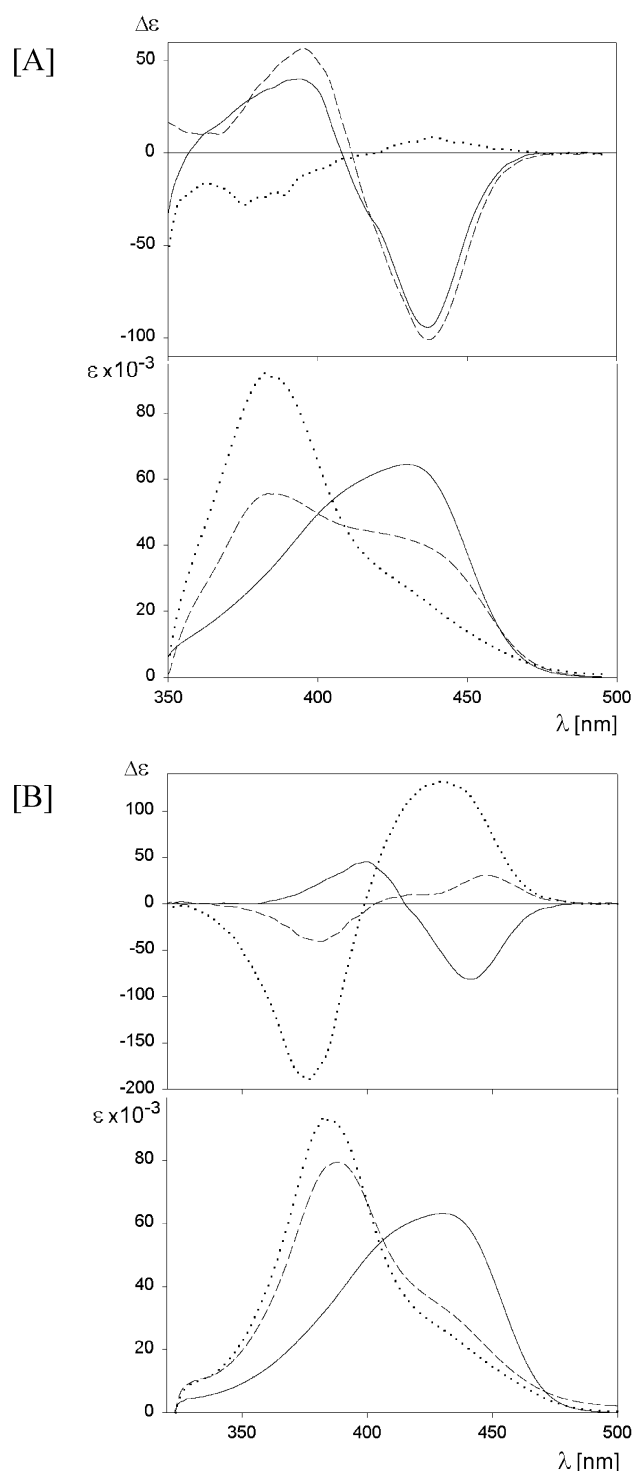


FIGURE 8. CD (upper) and UV-vis (lower) spectra of benzoic acid rubins **1o** (—), **1m** (---), and **1p** (····) in CHCl_3 with added quinine [A] and added cinchonidine [B]. The pigment/alkaloid ratio is 1:300 for pigment concentrations of $1.6\text{--}1.9 \times 10^{-5}$ M at 23 °C.

leads typically to an intense bisignate induced circular dichroism (ICD) Cotton effect, as has been noted previously for bilirubin in chloroform with added quinine^{34b} or other optically active amines^{38a-d,g-i} and in aqueous buffers with added serum albumin.³⁹ Similarly, for the benzoic acid rubins of **1o** and **1m** of this work, in CHCl_3 comparably intense negative exciton chirality ICDs are

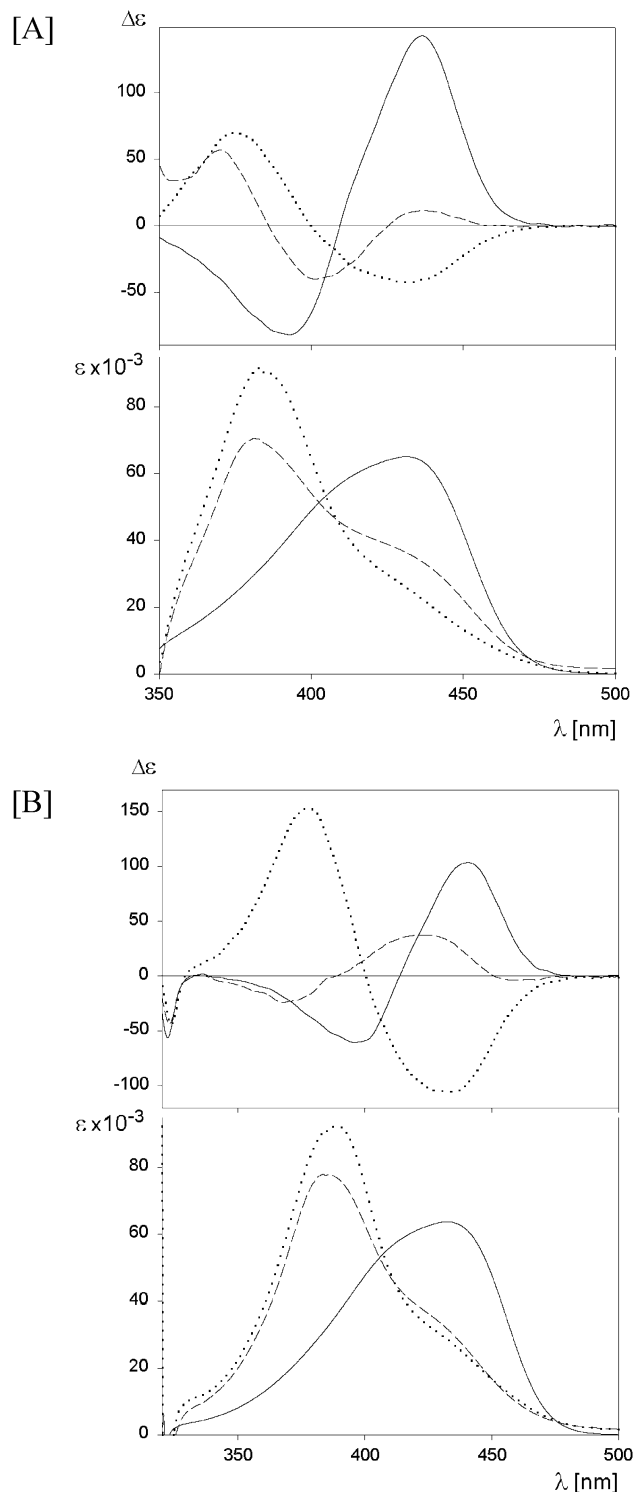


FIGURE 9. CD (upper) and UV-vis (lower) spectra of benzoic acid rubins **1o** (—), **1m** (---), and **1p** (····) in CHCl_3 with added quinidine [A] and added cinchonine [B]. The pigment/alkaloid ratio is 1:300 for pigment concentrations of $1.6\text{--}1.9 \times 10^{-5}$ M at 23 °C.

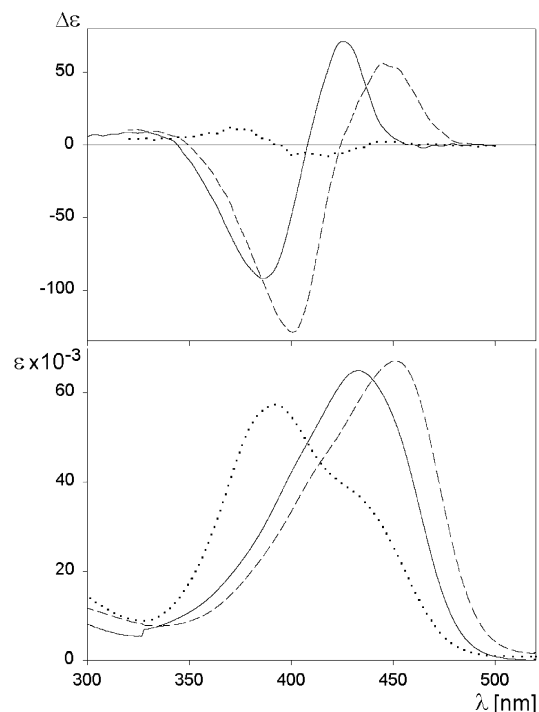
observed in the presence of quinine (Figure 8A), as is characteristic of an exciton system in which the two dipyrnone chromophores of the bichromophoric rubin molecule interact by coupling locally excited $\pi \rightarrow \pi^*$ transitions (electric dipole transition moment coupling).⁴⁰ In contrast, only a weaker, broader positive exciton

TABLE 6. Comparison of Circular Dichroism and UV-vis Spectral Data of Carboxyphenyl-mesobilirubins 1 in the Presence of Cinchona Alkaloids^a

pigment + alkaloid	CD			UV	
	$\Delta\epsilon_{\max} (\lambda_1)$	λ_2 at $\Delta\epsilon = 0$	$\Delta\epsilon_{\max} (\lambda_3)$	ϵ_{\max}	λ_{\max}
1o + quinine	-94.5 (437)	408	+40.0 (394)	64,500	430
1m + quinine	-101.2 (437)	411	+56.5 (395)	42,400 ^{sh}	427
1p + quinine	+8.6 (439)	419	-28.1 (376)	55,600	383
1o + quinidine	+142.9 (436)	410	-82.1 (393)	26,800 ^{sh}	430
1m + quinidine	-40.2 (401)	386	+56.9 (370)	92,200	383
1p + quinidine	-42.6 (432)	400	+70.1 (375)	65,100	431
1o + cinchonidine	-81.5 (441)	415	+45.4 (400)	38,500 ^{sh}	426
1m + cinchonidine	+30.6 (448)	403	-40.4 (381)	70,500	381
1p + cinchonidine	+132.1 (430)	399	-189.1 (377)	26,600 ^{sh}	430
1o + cinchonine	+103.7 (441)	414	-60.6 (396)	91,800	383
1m + cinchonine	+37.4 (425)	389	-24.1 (367)	63,200	431
1p + cinchonine	-105.4 (435)	400	+153.0 (378)	34,100 ^{sh}	427
				77,800	386
				29,600 ^{sh}	431
				92,300	386

^a Concentration $1.6\text{--}1.9 \times 10^{-5}$ M of a chloroform solution containing $4.8\text{--}5.7 \times 10^{-3}$ M concentration of each alkaloid.

chirality CD is observed for **1p**. The UV-vis curves also show evidence of exciton coupling, but the CD curves indicate chiral stereochemistry: a preponderance of the *M* helical rubin enantiomers **1o** and **1m** and a mild preference for *P* in **1p** due to enantioselection by quinine. Interestingly, in the presence of a related alkaloid (cinchonidine) with the same absolute configuration, only the CD and UV spectra (Figure 8B) of **1o** and the UV of **1p** remain relatively unchanged. The CD couplet of **1m** weakens and inverts signs and the UV spectrum shifts, whereas the CD of **1p** intensifies greatly to give a well-defined positive exciton chirality couplet. The exciton CD couplet signs of **1o** invert in the presence of quinidine and cinchonine (Figure 9) with UV-vis spectra remaining similar to those of Figure 8. With sign inversions, the CD spectra of **1p** remain similar to those in Figure 8A, and those in Figure 9B remain similar to those in Figure 8B. Oddly, the CD spectra (Figure 9) of **1m** vary considerably: those of Figure 8B and 9B are similar (as are the UVs), and those of Figure 8A and 9A have the same signed order but rather different magnitudes. Yet the UV-vis profiles for **1m** in Figures 8A and 9A remain similar. In some cases (quinidine, cinchonine) the magnitudes are larger; in others (cinchonidine) they are smaller, apparently all dictated by the stability of the complex formed. It is tempting to link the “well-behaved” exciton curves seen for **1o** to their ability to fold into ridge-tile conformations and maintain them by intramolecular hydrogen bonding. The CD curves of **1m** show nice behavior only with quinine; those of **1p** show intense bisignate Cotton effects only with cinchonidine and cinchonine. At present the reasons for the varying

**FIGURE 10.** CD (upper) and UV-vis (lower) spectra of $1.6\text{--}1.9 \times 10^{-5}$ M benzoic acid rubins **1o** (—), **1m** (---), and **1p** (····) in aqueous buffered (pH 7.4, Tris) human serum albumin (HSA) at 23 °C. The pigment/HSA ratio is 1:2.**TABLE 7. Comparison of Circular Dichroism and UV-vis Spectral Data of Carboxyphenyl-mesobilirubins 1 in the Presence of Human Serum Albumin^a**

pigment (buffer)	CD			UV	
	$\Delta\epsilon_{\max} (\lambda_1)$	λ_2 at $\Delta\epsilon = 0$	$\Delta\epsilon_{\max} (\lambda_3)$	ϵ_{\max}	λ_{\max}
1o (A)	+32.1 (425)	413	-80.9 (389)	64,700	437
1o (B)	+36.2 (429)	413	-83.1 (389)	65,800	437
1o (C)	+71.3 (425)	409	-92.0 (386)	65,000	433
1m (A)	+50.2 (448)	425	-116.2 (400)	65,800	451
				41,900 ^{sh}	413
1m (B)	+53.5 (448)	425	-124.7 (401)	65,200	451
				42,700 ^{sh}	415
1m (C)	+56.1 (445)	424	-129.0 (401)	67,100	451
				44,300 ^{sh}	414
1p (A)	-10.4 (417)	393	+11.2 (377)	34,500 ^{sh}	435
				60,300	389
1p (B)	-9.5 (398)	386	+6.4 (369)	34,100 ^{sh}	435
				60,500	390
1p (C)	-7.8 (418)	392	+12.0 (371)	36,500 ^{sh}	434
				57,300	392

^a Concentration of pigment $1.6\text{--}1.9 \times 10^{-5}$ M; concentration of HSA $3.2\text{--}3.8 \times 10^{-5}$ M. Buffers: A, 0.1 M phosphate buffer, pH 7.42; B, 0.1 M phosphate buffer, pH 8.02; C, 0.1 M Tris buffer, pH 7.40.

behaviors are not clear. The UV-vis curves of **1o** vary little from one alkaloid solution to another and differ from those of **1m** and **1p**. In Figures 8 and 9, the UV-vis curves of **1m** are very much like those of **1p**, showing a strong tilt toward the higher energy exciton component near 380 nm and are thus consistent with a conformation dominated by a more helix-like structure involved in intermolecular hydrogen bonding. The data are summarized in Table 6.

When human serum albumin (HSA) is used as the chiral complexation agent, aqueous buffered (pH 7.4 Tris

(40) Bauman, D.; Killet, C.; Boiadjev, S. E.; Lightner, D. A.; Schönhofer, A.; Kuball, H.-G. *J. Phys. Chem.* **1996**, *100*, 11546–11558.

or phosphate) solutions of **1o** and **1m** exhibit strong positive exciton chirality bisignate ICD Cotton effects, effectively the same as observed for bilirubin. In contrast, **1p** exhibits a much weaker negative chirality Cotton effect that is broadly bisignate (Figure 10). The CD intensities of **1** are comparable in magnitude to those of bilirubin, apparently due to a similar enantioselective chiral complexation by HSA. Interestingly, for reasons yet unclear, a change in pH, from 7.4 to 8.0 leads to more intense Cotton effects for both **1o** and **1m** but not for **1p**. The ICD data for **1o** and **1m** suggest rather similar conformations on HSA, whereas the contrasting ICD data for **1p** suggest a different conformation or a mixture of conformations.

Conclusions

Novel analogues (**1**) of bilirubin with propionic acids replaced by benzoic acids offer three different isomers and three different fixed orientations of the carboxylic acid groups relative to the two dipyrinone components of the pigment. In only one isomer, the *ortho* (**1o**), can intramolecular hydrogen bonding (Figure 3) effectively stabilize the ridge-tilt conformation. Consequently, **1o** is less polar than either the *meta* (**1m**) or *para* (**1p**) isomers and exhibits uniquely different chromatographic and spectroscopic properties.

Experimental Section

General Procedures. Nuclear magnetic resonance spectra were acquired at 11.75 T magnetic field strength instrument operating at ^1H frequency of 500 MHz and ^{13}C frequency of 125 MHz in solutions of CDCl_3 (referenced at 7.26 ppm for ^1H and 77.00 ppm for ^{13}C) or $(\text{CD}_3)_2\text{SO}$ (referenced at 2.49 ppm for ^1H and 39.50 ppm for ^{13}C). J -modulated spin-echo (Attached Proton Test) and gHMBC experiments were used to assign the ^{13}C NMR spectra. Gas chromatography-mass spectrometry analyses were carried out on a gas chromatograph (30 m DB-1 column) equipped with a mass selective detector. Radial chromatography was carried out on silica gel PF₂₅₄ with CaSO_4 binder preparative layer grade, using 1-, 2-, or 4-mm thick rotors, and analytical thin-layer chromatography was carried out on silica gel IB-F plates (125- μm layer). Melting points are uncorrected. The combustion analyses were carried out by Desert Analytics, Tucson, AZ. High-resolution FAB mass spectra were obtained at the Nebraska Center for Mass Spectrometry, University of Nebraska, Lincoln, for samples which were >98% pure by NMR.

The spectral data were obtained in spectral grade solvents, used as provided, and dimethylformamide was purified by a standard procedure.⁴¹

Methyl 3,5-Dimethyl-4-iodo-1H-pyrrole-2-carboxylate (11). According to Treibs and Kolm²⁶ for iodination of the ethyl ester of **10**, to a solution of 15.32 g (100 mmol) of methyl 3,5-dimethyl-1H-pyrrole-2-carboxylate (**10**)²⁵ in 150 mL of ethanol, 6 mL (105 mmol) of acetic acid, and 22 mL (200 mmol) of 30% aqueous hydrogen peroxide was added a solution of 18.26 g (110 mmol) of potassium iodide in 25 mL of water during 10 min at 75–80 °C. The mixture was stirred at 75 °C for 10 min. Then it was cooled slowly while adding 60 mL of water and chilled at –15 °C for 2 h. The product was collected by filtration, washed with cold aqueous ethanol, and dried under vacuum. Recrystallization from ethyl acetate–hexane afforded 26.12 g (94%) of iodopyrrole **11**: mp 188–189 °C; ^1H NMR (CDCl_3) δ 2.28 (3H, s), 2.29 (3H, s), 3.85 (3H, s), 9.14 (1H, br.

s) ppm; ^{13}C NMR (CDCl_3) δ 14.3, 14.6, 51.3, 72.1, 118.1, 130.9, 134.6, 161.6 ppm; MS m/z (relative abund.) 279 (M^+ , 100%), 247 (85%), 220 (9%), 120 (8%). Anal. Calcd for $\text{C}_8\text{H}_{10}\text{INO}_2$ (279.1): C, 34.43; H, 3.61; N, 5.02. Found: C, 34.38; H, 3.69; N, 4.94.

General Procedure for Syntheses of Arylpyrroles 8m and 8p. To an argon-protected solution of 2.79 g (10 mmol) of iodopyrrole **11** and 2.70 g (15 mmol) of boronic acid **12m**²³ or **12p**²⁴ in 70 mL of purified and deoxygenated dimethylformamide was added 462 mg (0.4 mmol) of $\text{Pd}(\text{PPh}_3)_4$ ²⁷ followed by a hot solution of 2.12 g (20 mmol) of anhydrous Na_2CO_3 in 13 mL of deoxygenated water. The mixture was placed in a preheated oil bath at 100–105 °C and stirred under Ar for 20–25 min (until sudden color change from yellow to dark brown-black). After cooling with an ice bath, the mixture was diluted with 350 mL of diethyl ether and washed with 10% aqueous NH_4OH (3×50 mL) and then with water (4×50 mL). The organic layer was dried (MgSO_4) and filtered, and the solvent was evaporated under vacuum. The residue was purified by radial chromatography (eluent hexane–ethyl acetate = 93:7 to 85:15) collecting the bright fluorescent band of arylpyrroles **8m** or **8p**. After solvent evaporation, the material was recrystallized from hexanes–ethyl acetate.

Methyl 3,5-Dimethyl-4-(*m*-methoxycarbonylphenyl)-1H-pyrrole-2-carboxylate (8m). The *meta*-isomer was obtained in 77% yield: mp 140–141 °C; ^1H NMR (CDCl_3) δ 2.25 (3H, s), 2.28 (3H, s), 3.87 (3H, s), 3.93 (3H, s), 7.43 (1H, m), 7.47 (1H, m), 7.93 (1H, m), 7.97 (1H, m), 8.78 (1H, br. s) ppm; ^{13}C NMR (CDCl_3) δ 11.3, 12.1, 51.1, 52.1, 117.4, 123.7, 126.6, 127.4, 128.3, 130.16, 130.21, 131.1, 134.5, 135.4, 162.2, 167.2 ppm; MS m/z (relative abund.) 287 (M^+ , 81%), 256 (44%), 255 (100%), 224 (9%), 195 (12%), 168 (31%). Anal. Calcd for $\text{C}_{16}\text{H}_{17}\text{NO}_4$ (287.3): C, 66.88; H, 5.96; N, 4.88. Found: C, 66.78; H, 5.74; N, 4.96.

Methyl 3,5-Dimethyl-4-(*p*-methoxycarbonylphenyl)-1H-pyrrole-2-carboxylate (8p). Following the procedure above, the *para*-isomer was synthesized in 78% yield: mp 155–156 °C; ^1H NMR (CDCl_3) δ 2.27 (3H, s), 2.30 (3H, s), 3.87 (3H, s), 3.94 (3H, s), 7.31 (2H, m, $^3J = 8.5$ Hz), 8.07 (2H, m, $^3J = 8.5$ Hz), 8.83 (1H, br. s) ppm; ^{13}C NMR (CDCl_3) δ 11.3, 12.2, 51.1, 52.0, 117.7, 123.7, 126.5, 127.8, 129.5, 129.8, 130.3, 140.1, 162.1, 167.1 ppm; MS m/z (relative abund.) 287 (M^+ , 94%), 255 (100%), 224 (25%), 196 (11%), 168 (21%). Anal. Calcd for $\text{C}_{16}\text{H}_{17}\text{NO}_4$ (287.3): C, 66.88; H, 5.96; N, 4.88. Found: C, 67.20; H, 6.02; N, 4.92.

3-Ethyl-8-(*o*-methoxycarbonylphenyl)-2,7,9-trimethyl-1,10-dihydro-11H-dipyrin-1-one (5o) was prepared as reported previously¹⁵ from reaction of **6** and **7o**: mp 289–291 °C (lit.¹⁵ mp 289–291 °C); UV–vis $\epsilon_{435}^{\text{sh}}$ 27,700, $\epsilon_{410}^{\text{max}}$ 45,900 (benzene), $\epsilon_{407}^{\text{max}}$ 40,500 (CHCl_3), $\epsilon_{413}^{\text{max}}$ 42,000 (CH_3OH), $\epsilon_{400}^{\text{max}}$ 38,100 (CH_3CN), $\epsilon_{412}^{\text{max}}$ 39,900, $\epsilon_{399}^{\text{max}}$ 38,100 (DMSO); ^{13}C NMR and ^1H NMR in Tables 1 and 2.

3-Ethyl-8-(*m*-methoxycarbonylphenyl)-2,7,9-trimethyl-1,10-dihydro-11H-dipyrin-1-one (5m). A mixture of 1.44 g (5 mmol) of monopyrrole **8m**, 2.00 g (50 mmol) of sodium hydroxide, 30 mL of ethanol, and 9 mL of water was heated at reflux for 4 h. After cooling, the ethanol solvent was evaporated under vacuum, and the residue was diluted with 10 mL of 50% aqueous NaNO_3 . The solution was cooled at –20 °C and acidified by slow addition of a solution of concentrated HNO_3 in 50% aqueous NaNO_3 (1:5 v/v). The precipitated product was collected by filtration, washed with cold water and dried overnight under vacuum. This crude diacid (**7m**) was obtained in nearly quantitative yield and was used immediately in the following step without further characterization.

A mixture of diacid from above, 1.17 g (5.4 mmol) of 5-bromomethylene-4-ethyl-3-methyl-2-oxo-1H-pyrrole (**6**),²⁸ 35 mL of anhydrous methanol, and 1 drop of 48% aqueous HBr was heated at reflux for 9 h. Then the mixture was chilled overnight at –20 °C. The precipitated crude dipyrinone acid **4m** was collected by filtration, suspended in 50 mL of CH_3OH

(41) Perrin, D. D.; Armarego, W. L. F. *Purification of Laboratory Chemicals*, 3rd ed.; Pergamon Press: England, 1988.

and 30 mL of CHCl_3 , and treated for 10 min with ethereal diazomethane (generated from 30 mmol of *N*-nitroso-*N*-methylurea). Excess CH_2N_2 was destroyed with acetic acid, and the solvents were evaporated under vacuum. The residue was purified by radial chromatography (2–4% CH_3OH in CHCl_3 – CH_2Cl_2 = 1:1 v/v) and after recrystallization from CH_2Cl_2 – CH_3OH , 1.36 g (75%) of bright yellow dipyrinone **5m** was obtained: mp 272–273 °C; UV–vis $\epsilon_{430}^{\text{max}}$ 30,300, $\epsilon_{408}^{\text{max}}$ 45,900 (benzene), $\epsilon_{405}^{\text{max}}$ 41,300 (CHCl_3), $\epsilon_{409}^{\text{max}}$ 42,500 (CH_3OH), $\epsilon_{397}^{\text{max}}$ 36,900 (CH_3CN), $\epsilon_{408}^{\text{max}}$ 40,000 (DMSO); ^1H NMR (CDCl_3) δ 1.21 (3H, t, J = 7.6 Hz), 1.97 (3H, s), 2.18 (3H, s), 2.48 (3H, s), 2.58 (2H, q, J = 7.6 Hz), 3.94 (3H, s), 6.22 (1H, s), 7.48 (1H, m), 7.49 (1H, m), 7.96 (1H, m), 7.98 (1H, m), 10.63 (1H, br. s), 11.39 (1H, br. s) ppm; ^{13}C NMR (CDCl_3) δ 8.6, 10.3, 12.3, 15.0, 18.0, 52.1, 101.0, 122.7, 122.9, 123.0, 123.8, 127.0, 127.9, 128.2, 130.2, 130.9, 131.9, 134.3, 136.2, 148.5, 167.3, 174.3 ppm. Anal. Calcd for $\text{C}_{22}\text{H}_{24}\text{N}_2\text{O}_3$ (364.4): C, 72.50; H, 6.64; N, 7.69. Found: C, 72.24; H, 6.48; N, 7.44.

3-Ethyl-8-(*p*-isobutoxycarbonylphenyl)-2,7,9-trimethyl-1,10-dihydro-11*H*-dipyrin-1-one (5p). Following the procedure from above 1.44 g (5 mmol) of monopyrrole **8p** was converted to 1.42 g (81%) of crude dipyrinone acid **4p** (containing ~10% of methyl ester). This amount was treated for 2 h at reflux with a mixture of 25 mL of 10% aqueous NaOH and 50 mL of ethanol. After cooling, the ethanol solvent was evaporated under vacuum. The residue was diluted with cold water (25 mL) and acidified at 0 °C with 10% aqueous HCl. The reprecipitated **4p** was collected by filtration, washed with water, and dried for 48 h under vacuum (P_2O_5).

A mixture of 1.30 g (3.7 mmol) of this purified acid, 1.79 g (5.5 mmol) of cesium carbonate, 30 mL of anhydrous dimethylformamide and 1.3 mL (11.1 mmol) of isobutyl iodide was heated for 18 h at 80 °C. After cooling the mixture was partitioned between 300 mL of CHCl_3 and 300 mL of H_2O . The organic layer was washed with water (3 \times 100 mL) and dried (Na_2SO_4), and after filtration, the solvent was evaporated under vacuum. The residue was purified by radial chromatography (eluent 2–3% CH_3OH in CH_2Cl_2) and the pure material was recrystallized from CH_3OH – CH_2Cl_2 to afford 1.18 g (58% based on **8p**) of bright yellow isobutyl ester **5p**: mp 263–264 °C; UV–vis $\epsilon_{431}^{\text{max}}$ 33,900, $\epsilon_{410}^{\text{max}}$ 49,000 (benzene), $\epsilon_{406}^{\text{max}}$ 43,900 (CHCl_3), $\epsilon_{411}^{\text{max}}$ 46,100 (CH_3OH), $\epsilon_{397}^{\text{max}}$ 40,400 (CH_3CN), $\epsilon_{412}^{\text{max}}$ 43,200, $\epsilon_{404}^{\text{sh}}$ 42,300 (DMSO); ^1H NMR (CDCl_3) δ 1.05 (6H, d, J = 6.7 Hz), 1.20 (3H, t, J = 7.7 Hz), 1.97 (3H, s), 2.11 (1H, m), 2.20 (3H, s), 2.50 (3H, s), 2.58 (2H, q, J = 7.7 Hz), 4.13 (2H, d, J = 6.5 Hz), 6.21 (1H, s), 7.37 (2H, d, J = 8.3 Hz), 8.09 (2H, d, J = 8.3 Hz), 10.65 (1H, br. s), 11.38 (1H, br. s) ppm; ^{13}C NMR (CDCl_3) δ 8.6, 10.4, 12.5, 15.0, 18.0, 19.2, 28.0, 70.9, 100.9, 122.8, 123.0, 123.2, 123.7, 127.8, 128.0, 129.5, 129.6, 132.1, 140.8, 148.6, 166.8, 174.3 ppm. Anal. Calcd for $\text{C}_{25}\text{H}_{30}\text{N}_2\text{O}_3$ (406.5): C, 73.86; H, 7.44; N, 6.89. Found: C, 74.22; H, 7.64; N, 6.90.

General Procedure for Syntheses of Dipyrinone Acids 4. A mixture of 1 mmol of the corresponding ester **5a**, **5m**, or **5p**, 10 mL of 10% aqueous NaOH, and 25 mL of ethanol was heated at reflux for 3 h. After cooling, the ethanol solvent was removed under vacuum. The residue was diluted with 10 mL of water and acidified at 0 °C with 10% aqueous HCl. The precipitated product was collected by filtration, washed with water (3 \times 10 mL), and dried under vacuum for 24 h (P_2O_5).

8-(*o*-Carboxyphenyl)-3-ethyl-2,7,9-trimethyl-1,10-dihydro-11*H*-dipyrin-1-one (4o). The acid **4o** was isolated in 94% yield. It decomposed without melting at 287–314 °C; UV–vis $\epsilon_{405}^{\text{max}}$ 35,900 (benzene), $\epsilon_{405}^{\text{max}}$ 35,000 (CHCl_3), $\epsilon_{411}^{\text{max}}$ 36,000 (CH_3OH), $\epsilon_{398}^{\text{max}}$ 35,400 (CH_3CN), $\epsilon_{405}^{\text{max}}$ 35,100 (DMSO); NMR data in Tables 1 and 2; HRMS (FAB, 3-NBA) calcd for $\text{C}_{21}\text{H}_{22}\text{N}_2\text{O}_3$ 350.1630; found 350.1635, Δ = –0.5 mDa, error –1.3 ppm.

8-(*m*-Carboxyphenyl)-3-ethyl-2,7,9-trimethyl-1,10-dihydro-11*H*-dipyrin-1-one (4m). Following the general procedure above, acid **4m** was obtained in 98% yield. It decom-

posed without melting at 309–331 °C; UV–vis $\epsilon_{415}^{\text{max}}$ 38,000, $\epsilon_{401}^{\text{max}}$ 37,400 (benzene), $\epsilon_{408}^{\text{max}}$ 38,300 (CHCl_3), $\epsilon_{411}^{\text{max}}$ 39,100 (CH_3OH), $\epsilon_{400}^{\text{max}}$ 37,400 (CH_3CN), $\epsilon_{409}^{\text{max}}$ 37,000 (DMSO); NMR data in Tables 1 and 2; HRMS (FAB, 3-NBA) calcd for $\text{C}_{21}\text{H}_{22}\text{N}_2\text{O}_3$ 350.1630; found 350.1628, Δ = 0.2 mDa, error 0.6 ppm.

8-(*p*-Carboxyphenyl)-3-ethyl-2,7,9-trimethyl-1,10-dihydro-11*H*-dipyrin-1-one (4p). This dipyrinone acid was prepared in 95% yield. It decomposed without melting at 322–343 °C; UV–vis $\epsilon_{416}^{\text{max}}$ 39,600, $\epsilon_{401}^{\text{max}}$ 39,100 (benzene), $\epsilon_{408}^{\text{max}}$ 39,800 (CHCl_3), $\epsilon_{411}^{\text{max}}$ 41,000 (CH_3OH), $\epsilon_{398}^{\text{max}}$ 39,900 (CH_3CN), $\epsilon_{411}^{\text{max}}$ 38,100, $\epsilon_{403}^{\text{sh}}$ 37,500 (DMSO); NMR data in Tables 1 and 2; HRMS (FAB, 3-NBA) calcd for $\text{C}_{21}\text{H}_{22}\text{N}_2\text{O}_3$ 350.1630; found 350.1629, Δ = 0.1 mDa, error 0.3 ppm.

General Procedure for Syntheses of Mesobiliverdin Esters Analogues 3. To a solution of 2.00 mmol of the corresponding dipyrinone ester (**5a**, **5m** or **5p**) in 440 mL of CH_2Cl_2 was added *p*-chloranil (1.23 g, 5.00 mmol) followed by 22 mL of 97% formic acid, and the mixture was heated at reflux for 24 h. The reaction volume was reduced by distillation to one-half, and reflux was continued for 6 h. Then the mixture was chilled overnight at –20 °C. The separated yellow solid was removed by filtration and discarded. The blue filtrate was carefully neutralized with 5% aqueous NaHCO_3 and then washed with 4% aqueous NaOH (2 \times 100 mL) and H_2O (4 \times 100 mL). After drying (anhydrous Na_2SO_4), filtration, and evaporation of the solvent under vacuum, the residue was purified by radial chromatography (gradient CH_2Cl_2 – $\text{CH}_3\text{CO}_2\text{H}$ – CH_3OH = 100:3.2 to 100:3:7 v/v/v). The combined pure fractions were washed with 1% aqueous NaHCO_3 and H_2O and then dried (anhydrous Na_2SO_4). After filtration, the solvent was evaporated under vacuum and the residue was recrystallized from CHCl_3 –hexane to afford pure mesobiliverdin esters **3**.

3,17-Diethyl-8,12-bis(*o*-methoxycarbonylphenyl)-2,7,13,18-tetramethyl-(21*H*,24*H*)-bilin-1,19-dione (3o). This mesobiliverdin ester was synthesized in 84% yield as previously described from dipyrinone **5a**:¹⁵ mp 284–288 °C (lit.¹⁵ mp 284–8 °C); UV–vis $\epsilon_{650}^{\text{max}}$ 18,300, $\epsilon_{375}^{\text{max}}$ 65,100 (benzene), $\epsilon_{646}^{\text{max}}$ 17,200, $\epsilon_{375}^{\text{max}}$ 66,400 (CHCl_3), $\epsilon_{648}^{\text{max}}$ 17,100, $\epsilon_{370}^{\text{max}}$ 66,300 (CH_3OH), $\epsilon_{647}^{\text{max}}$ 17,400, $\epsilon_{367}^{\text{max}}$ 67,700 (CH_3CN), $\epsilon_{648}^{\text{max}}$ 19,500, $\epsilon_{375}^{\text{max}}$ 66,400 (DMSO).

3,17-Diethyl-8,12-bis(*m*-methoxycarbonylphenyl)-2,7,13,18-tetramethyl-(21*H*,24*H*)-bilin-1,19-dione (3m). This mesobiliverdin ester was synthesized in 85% yield: mp 269–271 °C; UV–vis $\epsilon_{647}^{\text{max}}$ 19,900, $\epsilon_{375}^{\text{max}}$ 67,500 (benzene), $\epsilon_{639}^{\text{max}}$ 18,100, $\epsilon_{375}^{\text{max}}$ 70,100 (CHCl_3), $\epsilon_{638}^{\text{max}}$ 18,500, $\epsilon_{370}^{\text{max}}$ 71,000 (CH_3OH), $\epsilon_{632}^{\text{max}}$ 18,200, $\epsilon_{366}^{\text{max}}$ 70,500 (CH_3CN), $\epsilon_{630}^{\text{max}}$ 22,500, $\epsilon_{375}^{\text{max}}$ 68,100 (DMSO); ^1H NMR (CDCl_3) δ 1.24 (6H, t, J = 7.6 Hz), 1.84 (6H, s), 2.14 (6H, s), 2.54 (4H, q, J = 7.6 Hz), 3.93 (6H, s), 6.00 (2H, s), 6.47 (1H, s), 7.45 (2H, m), 7.48 (2H, m), 7.96 (2H, m), 7.97 (2H, m), 8.47 (2H, br. s) ppm; ^{13}C NMR (CDCl_3) δ 8.4, 10.2, 14.4, 17.9, 52.2, 96.1, 118.5, 127.9, 128.4, 128.5, 128.8, 130.4, 130.8, 134.0, 134.2, 139.3, 140.6, 141.5, 146.8, 150.0, 166.8, 172.6 ppm. Anal. Calcd for $\text{C}_{43}\text{H}_{42}\text{N}_4\text{O}_6$ (710.8): C, 72.66; H, 5.96; N, 7.88. Found: C, 72.49; H, 5.78; N, 7.88.

3,17-Diethyl-8,12-bis(*p*-isobutoxycarbonylphenyl)-2,7,13,18-tetramethyl-(21*H*,24*H*)-bilin-1,19-dione (3p). This compound was obtained in 80% yield: mp 265–266 °C; UV–vis $\epsilon_{654}^{\text{max}}$ 19,700, $\epsilon_{378}^{\text{max}}$ 70,300 (benzene), $\epsilon_{651}^{\text{max}}$ 18,200, $\epsilon_{375}^{\text{max}}$ 74,300 (CHCl_3), $\epsilon_{644}^{\text{max}}$ 18,500, $\epsilon_{371}^{\text{max}}$ 77,300 (CH_3OH), $\epsilon_{639}^{\text{max}}$ 18,400, $\epsilon_{371}^{\text{max}}$ 76,200 (CH_3CN), $\epsilon_{637}^{\text{max}}$ 21,700, $\epsilon_{378}^{\text{max}}$ 72,100 (DMSO); ^1H NMR (CDCl_3) δ 1.03 (12H, d, J = 6.7 Hz), 1.24 (6H, t, J = 7.6 Hz), 1.83 (6H, s), 2.10 (2H, m), 2.14 (6H, s), 2.54 (4H, q, J = 7.6 Hz), 4.12 (4H, d, J = 6.6 Hz), 6.02 (2H, s), 6.53 (1H, s), 7.34 (4H, d, J = 8.2 Hz), 8.08 (4H, d, J = 8.2 Hz), 8.40 (2H, br. s) ppm; ^{13}C NMR (CDCl_3) δ 8.3, 10.3, 14.4, 17.9, 19.2, 27.9, 71.1, 95.9, 118.4, 128.3, 128.8, 129.4, 129.66, 129.70, 138.4, 139.4, 140.6, 141.5, 146.8, 150.0, 166.3, 172.5 ppm. Anal. Calcd for $\text{C}_{49}\text{H}_{54}\text{N}_4\text{O}_6$ (795.0): C, 74.03; H, 6.85; N, 7.05. Found: C, 74.00; H, 6.78; N, 7.00.

General Procedure for Syntheses of Mesobilirubin Ester Analogues (2). To an oxygen-free solution of 0.5 mmol of the corresponding mesobiliverdin ester (**3o**, **3m**, or **3p**) in 8 mL of CHCl_3 and 80 mL of anhydrous CH_3OH kept at $\sim 10^\circ\text{C}$ was slowly added sodium borohydride (1.13 g, 30.0 mmol) during 15 min while purging the mixture with N_2 . After the mixture had turned from deep blue to bright yellow, ice–water (250 mL) was added, and the reaction was quenched with 8 mL of acetic acid followed by enough 10% aqueous HCl to bring the pH to ~ 3 . The product was extracted with CHCl_3 (4×100 mL), and the combined extracts were washed with water until neutral. After drying (anhydrous Na_2SO_4) and evaporation of the solvent under vacuum, the residue was purified by radial chromatography (gradient 0.5–3.0% of CH_3OH in CH_2Cl_2 v/v) and recrystallization from CH_2Cl_2 – CH_3OH to afford pure bright yellow mesobilirubin esters **2**.

3,17-Diethyl-8,12-bis(o-methoxycarbonylphenyl)-2,7,13,18-tetramethyl-(10H,21H,23H, 24H)-bilin-1,19-dione (2o). This mesobilirubin ester was synthesized in 92% yield as previously described.¹⁵

3,17-Diethyl-8,12-bis(m-methoxycarbonylphenyl)-2,7,13,18-tetramethyl-(10H,21H,23H, 24H)-bilin-1,19-dione (2m). This mesobilirubin ester was synthesized in 93% yield: mp 249–251 $^\circ\text{C}$ (decomp); ^1H NMR (CDCl_3) δ 1.06 (6H, t, $J = 7.6$ Hz), 1.60 (6H, s), 2.06 (6H, s), 2.39 (4H, q, $J = 7.6$ Hz), 3.93 (6H, s), 4.22 (2H, s), 6.02 (2H, s), 7.13 (4H, m), 7.80 (4H, m), 10.68 (2H, br. s), 10.87 (2H, br. s) ppm; ^{13}C NMR (CDCl_3) δ 8.0, 10.3, 14.8, 17.9, 23.3, 52.0, 100.4, 122.6, 123.0, 123.9, 124.3, 127.0, 128.1, 129.5, 129.8, 130.9, 131.0, 134.7, 135.8, 147.3, 167.2, 174.6 ppm. Anal. Calcd for $\text{C}_{43}\text{H}_{44}\text{N}_4\text{O}_6$ (712.8): C, 72.45; H, 6.22; N, 7.86. Found: C, 72.16; H, 6.07; N, 7.71.

3,17-Diethyl-8,12-bis(p-isobutoxycarbonylphenyl)-2,7,13,18-tetramethyl-(10H,21H,23H,24H)-bilin-1,19-dione (2p). This compound was obtained in 91% yield: mp 278–282 $^\circ\text{C}$ (decomp); ^1H NMR (CDCl_3) δ 1.05 (6H, t, $J = 7.7$ Hz), 1.06 (12H, d, $J = 6.7$ Hz), 1.54 (6H, s), 2.11 (6H, s), 2.12 (2H, m), 2.39 (4H, q, $J = 7.7$ Hz), 4.12 (4H, d, $J = 6.6$ Hz), 4.25 (2H, s), 6.03 (2H, s), 7.18 (4H, br. d, $J = 8.0$ Hz), 7.86 (4H, br. d, $J = 8.0$ Hz), 10.72 (2H, s), 10.90 (2H, s) ppm; ^{13}C NMR (CDCl_3) δ 7.8, 10.4, 14.8, 17.8, 19.3, 23.8, 27.9, 70.8, 100.3, 122.4, 123.3, 124.0, 124.6, 127.9, 129.3, 129.7, 129.8, 130.9, 140.3, 147.4, 166.4, 174.5 ppm. Anal. Calcd for $\text{C}_{49}\text{H}_{56}\text{N}_4\text{O}_6$ (797.0): C, 73.84; H, 7.08; N, 7.03. Found: C, 74.17; H, 7.00; N, 7.06.

General Procedure for Syntheses of Mesobilirubin Analogues (1). A mixture of 0.2 mmol of mesobilirubin diester **2o**, **2m**, or **2p** and 20 mL of ethanol was saturated for 30 min with argon. Then 3.0 mL of 1 M aqueous NaOH (3 mmol) was added and the mixture was heated at reflux for 1 h. In the case of the *ortho*-isomer (**1o**), after cooling the mixture was diluted with 100 mL of H_2O and 100 mL of CHCl_3 and then poured into 100 mL of 1% aqueous HCl, and the product was extracted with CHCl_3 (4×25 mL). The combined extracts were washed with H_2O (4×50 mL) and dried (anhydrous Na_2SO_4). After filtration and evaporation of the solvent under vacuum, the residue was purified by radial chromatography (gradient

1–2% of CH_3OH in CH_2Cl_2 v/v) and recrystallized from CH_3OH – CH_2Cl_2 to afford bright yellow **1o**. In the cases of much less soluble *meta* (**1m**) and *para* (**1p**) isomers, the ethanol solvent was partially (15 mL) removed by distillation while simultaneously adding 10 mL of water. After cooling, the mixture was further diluted with 20 mL of H_2O and slowly acidified at 0°C with 10% aqueous HCl until pH ~ 3 . The precipitated product was separated by filtration (or centrifugation), washed with H_2O (5×5 mL), and dried under vacuum to afford an almost quantitative yield of dark green **1m** or **1p**. Recrystallization from warm $(\text{CH}_3)_2\text{SO}$ – CHCl_3 afforded pure yellow rubins **1m** and **1p**.

8,12-Bis(o-carboxyphenyl)-3,17-diethyl-2,7,13,18-tetramethyl-(10H,21H,23H,24H)-bilin-1,19-dione (1o). This mesobilirubin was synthesized in 91% yield as previously described.¹⁵

8,12-Bis(m-carboxyphenyl)-3,17-diethyl-2,7,13,18-tetramethyl-(10H,21H,23H,24H)-bilin-1,19-dione (1m). This mesobilirubin was obtained in 55% yield. It decomposed at $>318^\circ\text{C}$; ^1H NMR ($(\text{CD}_3)_2\text{SO}$) δ 1.10 (6H, t, $J = 7.6$ Hz), 1.79 (6H, s), 1.89 (6H, s), 2.50 (4H, q, $J = 7.6$ Hz), 4.03 (2H, s), 5.91 (2H, s), 7.16 (2H, m), 7.27 (2H, m), 7.54 (2H, m), 7.68 (2H, m), 9.72 (2H, s), 10.39 (2H, s), 12.73 (2H, br. s) ppm; ^{13}C NMR ($(\text{CD}_3)_2\text{SO}$) δ 8.1, 9.9, 14.8, 17.2, 23.9, 97.5, 120.8, 122.4, 122.9, 123.6, 126.4, 127.8, 129.2, 129.6, 130.1, 130.3, 133.6, 135.2, 147.2, 167.3, 172.1 ppm. Anal. Calcd for $\text{C}_{41}\text{H}_{40}\text{N}_4\text{O}_6$ (684.8): C, 71.91; H, 5.89; N, 8.18. Found: C, 71.64; H, 6.01; N, 8.13.

8,12-Bis(p-carboxyphenyl)-3,17-diethyl-2,7,13,18-tetramethyl-(10H,21H,23H,24H)-bilin-1,19-dione (1p). This compound was prepared in 62% yield. It decomposed at $>328^\circ\text{C}$; ^1H NMR ($(\text{CD}_3)_2\text{SO}$) δ 1.09 (6H, t, $J = 7.5$ Hz), 1.79 (6H, s), 1.93 (6H, s), 2.50 (4H, q, $J = 7.5$ Hz), 4.06 (2H, s), 5.93 (2H, s), 7.06 (4H, d, $J = 8.0$ Hz), 7.75 (4H, d, $J = 8.0$ Hz), 9.76 (2H, s), 10.46 (2H, s), 12.66 (2H, br. s) ppm; ^{13}C NMR ($(\text{CD}_3)_2\text{SO}$) δ 8.1, 10.1, 14.8, 17.2, 24.1, 97.3, 120.6, 122.4, 123.2, 123.8, 127.7, 128.8, 129.2, 129.6, 129.8, 130.7, 147.2, 167.2, 172.1 ppm. Anal. Calcd for $\text{C}_{41}\text{H}_{40}\text{N}_4\text{O}_6$ (684.8): C, 71.91; H, 5.89; N, 8.18. Found: C, 72.12; H, 5.95; N, 8.14.

Acknowledgment. We thank the U.S. National Institutes of Health (HD-17779) for support of this work. S.E.B. is on leave from the Institute of Organic Chemistry, Bulgarian Academy of Sciences, Sofia.

Supporting Information Available: ^1H and ^{13}C NMR spectra, 500 and 125 MHz, respectively, of compounds **1o**, **1m**, and **1p** in $(\text{CD}_3)_2\text{SO}$ and **1o** in CDCl_3 ; compounds **2o**, **2m**, **2p**, **3o**, **3m**, **3p**, **5o**, **5m**, **5p**, **8m**, and **8p** in CDCl_3 ; compounds **4o**, **4m**, and **4p** in $(\text{CD}_3)_2\text{SO}$; and compound **7o** in $(\text{CD}_3)_2\text{SO}$. This material is available free of charge via the Internet at <http://pubs.acs.org>.

JO030091T